

1 **Late Weichselian and Holocene paleoceanography of Storfjordrenna, southern Svalbard**

2  
3 M. Łacka\*, M. Zajączkowski\*, M. Forwick\*\*, W. Szczuciński\*\*\*

4  
5 \*Institute of Oceanology, Polish Academy of Sciences, Powstańców Warszawy 55, 81-712  
6 Sopot, Poland.

7 \*\*Department of Geology, University of Tromsø – The Arctic University of Norway, N-9037  
8 Tromsø, Norway

9 \*\*\*Institute of Geology, Adam Mickiewicz University in Poznan, Maków Polnych 16, 61-  
10 606 Poznań, Poland

11  
12 Correspondence address: Magdalena Łacka, Institute of Oceanology, Polish Academy of  
13 Sciences, Powstańców Warszawy 55, 81-712 Sopot, Poland, e-mail: [mlacka@iopan.gda.pl](mailto:mlacka@iopan.gda.pl)

35           **Abstract**

36

37           Multiproxy analyses (incl. benthic and planktonic foraminifera,  $\delta^{18}\text{O}$  and  $\delta^{13}\text{C}$  records,  
38 grain-size distribution, ice-rafted debris, XRF geochemistry and magnetic susceptibility) were  
39 performed on a  $^{14}\text{C}$  dated marine sediment core from Storfjordrenna, off southern Svalbard.  
40 The sediments in the core cover the termination of Bølling-Allerød, the Younger Dryas and  
41 the Holocene, and they reflect general changes in the oceanography/climate of the European  
42 Arctic after the last glaciation. Grounded ice of the last Svalbard- Barents Sea Ice Sheet  
43 retreated from the coring site c. 13,950 cal yr BP. During the transition from the sub-glacial to  
44 glaciomarine setting, Arctic Waters dominated the hydrography in Storfjordrenna. However,  
45 the waters were not uniformly cold and experienced several warmer spells. A progressive  
46 warming and marked change in the nature of hydrology occurred during the early Holocene.  
47 Relatively warm and saline Atlantic Water started to dominate the hydrography from approx.  
48 9600 cal yr BP. Even though the climate in eastern Svalbard was milder at that time than at  
49 present (smaller glaciers), there were two slight coolings observed in the periods of 9000 -  
50 8000 cal yr BP and 6000 - 5500 cal yr BP. A change of the Storfjordrenna oceanography  
51 occurred at the beginning of late Holocene (i.e. 3600 cal yr BP) synchronously with glacier  
52 growth on land and enhanced bottom current velocities. Although cooling was observed in the  
53 surface water, Atlantic Water remained present in the deeper part of water column of  
54 Storfjordrenna.

55

56

57

58

59

60

61

62

63

## 64 **1 Introduction**

65

66 The northward flowing North Atlantic Current (NAC) is the most important source of heat  
67 and salt in the Arctic Ocean (Gammelsrod and Rudels, 1983; Aagaard et al., 1987; Schauer et  
68 al., 2004; Fig. 1b). The main stream of Atlantic Water (AW) flowing north to Fram Strait as  
69 the West Spitsbergen Current (WSC) causes the dramatic reduction of sea ice extent and  
70 thickness through the warming of the intermediate water layer in this region of the Arctic  
71 Ocean (Quadfasel et al., 1991; Serreze et al., 2003). Paleoceanographic (e.g., Spielhagen et  
72 al., 2011; Dylmer et al., 2013) and instrumental (Walczowski and Piechura 2006, 2007;  
73 Walczowski et al., 2012) investigations provide evidence of a recent intensification of the  
74 flow of AW in the Nordic Seas and the Fram Strait.

75 The Svalbard archipelago is influenced by two water masses: AW flowing northward from  
76 the North Atlantic and Arctic Water (ArW) flowing southwest from the northern Barents Sea  
77 (Fig. 1b). An oceanic front arising at the contact of different bodies of water is an excellent  
78 area to research contemporary and past environmental changes. Intensification of AW flow  
79 and associated climate warming cause decreased sea-ice cover in the Svalbard fjords during  
80 winter (Berge et al., 2006), increased sediment accumulation rate (Zajaczkowski et al., 2004;  
81 Szczuciński et al., 2009) and influences pelage-benthic carbon cycling (Zajaczkowski et al.,  
82 2010).

83 Paleoceanographic records indicate that AW was present along the western margin of  
84 Svalbard, at least, during the last 12,000 years (e.g. Ślubowska et al., 2007; Werner et al.,  
85 2011; Rasmussen et al., 2013); occasionally reaching the Hinlopen Trough and Kvitøya  
86 Trough, thus transporting warmer and more saline water to the eastern part of Svalbard from  
87 the north (Ślubowska-Woldengen et al., 2007; Ślubowska et al., 2008; Kubischta et al., 2010;  
88 Klitgaard Kristensen et al., 2013). Periods of enhanced inflow of AW during the Holocene led  
89 to the expansion of marine species being absent or only rarely occurring at present. This  
90 includes the mollusc *Mytilus edulis* whose fossil remains are widely distributed in raised  
91 beach deposits on the western and northern coasts of Svalbard (e.g. Feyling-Hanssen and  
92 Jørstad, 1950; Hjort et al., 1992). *Mytilus edulis* spawn at temperatures above 8 to 10 °C  
93 (Thorarinsdóttir and Gunnarson, 2003) and thus is considered to indicate higher surface-water  
94 temperature related to stronger AW inflow during the early Holocene (11,000 – 6800 cal yr  
95 BP) (Feyling-Hanssen, 1955; Salvigsen et al., 1992; Hansen et al., 2011). Although the  
96 progressive development of *Mytilus edulis* is well documented by the periods of warming and  
97 inflow of AW to Hinlopen Trough, the presence of this species in Storfjorden (W Edgeøya;

98 Fig. 1) is unclear. Hansen et al. (2011) suggested that a small branch of warm AW could have  
99 reached eastern Spitsbergen from the south at that time.

100 In the 1980s and 1990s, Storfjorden was regarded to be exclusively influenced by the East  
101 Spitsbergen Current (ESC), carrying the cold and less saline ArW from the Barents Sea  
102 (Quadfasel et al., 1988; Piechura et al., 1996). More recent studies suggested that the  
103 hydrography in Storfjorden is affected by the production of brine-enriched shelf waters (e.g.,  
104 Haarpaintner et al., 2001; Rasmussen and Thomsen, 2009), the creation of a coastal polynya  
105 (e.g., Skogseth et al., 2005; Geyer et al., 2010) or the overflow of dense waters to the  
106 continental shelf (e.g., Fer et al., 2003). However, hydrological data obtained from  
107 conductivity-temperature sensors attached to a *Delphinapterus leucas* showed a substantial  
108 and topographically steered inflow of AW to Storfjorden through the Storfjordrenna  
109 (Lydersen et al., 2002). Recently, Akimova et al. (2011) reviewed typical water masses for  
110 Storfjorden, where the AW was located between 50 and 70 meters.

111 Storfjordrenna is a sensitive boundary area (Fig. 1) where two contrasting water masses  
112 form an oceanic polar front, separating colder, less saline and isotopically lighter ArW from  
113 warmer, high saline and  $\delta^{18}\text{O}$  heavier AW. An abrupt cooling (e.g. Younger Dryas, Little Ice  
114 Age) and warming (e.g. early Holocene warming) of the European Arctic might be linked to  
115 relatively small displacements of this front (Sarnthein et al., 2003; Hald et al., 2004;  
116 Rasmussen et al., 2014).

117 Two sediment cores taken at the mouth of Storfjordrenna, reveal a continuous inflow of  
118 AW to the south western Svalbard shelf since the deglaciation of Svalbard-Barents Ice Sheet  
119 (Rasmussen et al., 2007), while inner Storfjorden basins undergo a shift from being occupied  
120 by continental ice to ice proximal condition (Rasmussen and Thomsen, in press). Nevertheless  
121 a limited amount of paleoceanographical data is available from this region, thus the  
122 reconstruction of the Svalbard-Barents Ice Sheet retreat and further development of  
123 Storfjordrenna oceanography is often speculative.

124 In this paper we present results from multi-proxy analyses of a sediment core retrieved  
125 100 km east of the mouth of Storfjordrenna (Fig. 1a). We provide a new age for the retreat of  
126 the last Svalbard-Barents Sea Ice Sheet from Storfjordrenna and discuss the interaction of  
127 oceanography and deglaciation, as well as the postglacial history of Atlantic Water inflow  
128 onto the shelf off southern Svalbard. Since the studied sediment core was retrieved from an  
129 oceanographic frontal zone, sensitive to larger-scale changes, we believe that the presented  
130 data show the general climatic/oceanographic trends in the eastern Arctic.

131

## 132 **2 Study area**

133

134 Storfjorden is an approx. 190 km long and up to 190 m deep glacial trough located  
135 between the landmasses of Spitsbergen to the west, Edgeøya and Barentsøya to the east, and  
136 the shallow Storfjordenbanken to the south-east (Fig. 1a). It is not a fjord *sensu stricto*, as the  
137 sounds of Heleysundet and Freemansundet to the north and northeast, respectively, connect  
138 the head of Storfjorden to the north western Barents Sea. A sill of 120 m depth crosses the  
139 mouth of Storfjorden. The 254 km long Storfjordrenna, a continuation of the trough that  
140 extends towards the shelf break, is located beyond this sill. Bottom depth along the trough  
141 axis varies between 150 m and 420 m (Pedrosa et al., 2011).

142

### 143 **2.1 Water masses**

144

145 The water column of Storfjorden and Storfjordrenna is composed of two main water  
146 masses transported with currents from east and south and mixed waters which are formed  
147 locally (Table 1. after Skogseth et al., 2005). Warm and saline Atlantic Water (AW) enters  
148 Storfjordrenna in a cyclonic manner (Schauer, 1995; Fer et al., 2003), flowing into the trough  
149 parallel to its southern margin and flowing towards the trough mouth along its northern slope.  
150 The AW occurs between 50 and 70 m in Storfjorden and extends to a depth of 200 m in  
151 Storfjordrenna (Akimova et al., 2011). The origin of AW entering Storfjordrenna is an  
152 eastward branch of the North Atlantic Current (NAC) following the topography of the Barents  
153 Sea Shelf Break. However, approx. 50% of AW flowing northward also penetrate into  
154 Bjørnøyrenna (Smedsrud et al., 2013; for location see Fig. 1). The AW in Storfjordrenna is  
155 cooler and fresher than in Bjørnøyrenna as an effect of distance and mixing processes  
156 (O'Dwyer et al., 2001). AW may occasionally propagate even further east of Svalbard, where  
157 it fills the depressions below 180 m (Schauer, 1995). Relatively cold Arctic Water (ArW) is  
158 transported to Storfjorden and Storfjordrenna by the East Spitsbergen Current (ESC). The  
159 ESC enters the fjord through the tidally influenced sounds of Heleysundet and Freemansundet  
160 in the north and northeast (Norges Sjøkartverk, 1988), as well as from the southeast with a  
161 coastal current flowing around Edgøya (Loeng, 1991). AW and ArW mix to form  
162 Transformed Atlantic Water (TAW), which dominates on the shelf off west Spitsbergen  
163 (Svendsen et al., 2002; Table 1). Dense, brine-enriched Shelf Water (BSW) in Storfjorden is  
164 produced through high polynya activity and results from intense formation of sea ice  
165 (Haarpaintner et al., 2001; Skogseth et al., 2004, 2005). The BSW fills the fjord to the top of

166 the sill (120 m) and initiates a gravity driven overflow (Quadfasel et al., 1988; Schauer, 1995;  
167 Schauer and Fahrbach, 1999; Fer et al., 2003, 2004; Skogseth et al., 2005). BSW is  
168 characterized by salinity greater than 34.8 and temperature at or slightly above the freezing  
169 point (Table 1). Surface Water (SW) in the upper 50 m is cold and fresh during the autumn  
170 and warm and fresh due to ice melting during the summer. In winter, the water column in  
171 Storfjorden is homogenized due to wind and tidal mixing and is considered to be close to the  
172 freezing point (Skogseth et al., 2005).

### 173 **3 Material and methods**

174

175 Multi-proxy analyses of the gravity core JM09-020-GC provided the basis for this study.  
176 The core was retrieved with R/V Jan Mayen (University of Tromsø – The Arctic University of  
177 Norway, UiT) in November 2009 from the Storfjordrenna (76°31489' N, 19°69957' E), from  
178 a bottom depth of 253 m (Fig. 1a). The coring site was located in an area above the  
179 continuous presence of BSW and was selected after an echo-acoustic investigation in order to  
180 identify the greatest possible area of flat bottom with minimum disturbance of sediments.  
181 Conductivity-temperature-depth (CTD) measurements were performed prior to coring (Fig.  
182 2a) and in summer 2013 (Fig. 2b).

183 Prior to sediment core opening, the magnetic susceptibility (MS) was measured using a  
184 loop sensor installed on a GEOTEK Multi Sensor Core Logger at the Department of Geology,  
185 UiT. Core sections were stored in the laboratory for one day before measurements thereby  
186 allowing the sediments to adjust to room temperature and to avoid measurement errors related  
187 to temperature changes (Weber et al., 1997). X-radiographs and digital images were taken  
188 from half of the core to define sedimentary and biogenic structures. Sediment colour was  
189 defined according to the Munsell Soil Color Charts (Munsell Products, 2009). Qualitative  
190 element-geochemical measurements were performed with an Avaatech X-ray fluorescence  
191 (XRF) core scanner using the following settings: 10 kV; 1000  $\mu$ A; 10 sec. measuring time; no  
192 filter. Both core halves were subsequently cut into 1-cm slices and transported to the Institute  
193 of Oceanology, Polish Academy of Sciences in Sopot for further analyses.

194 Sediment samples for foraminiferal analyses were freeze-dried, weighed, and wet sieved  
195 using sieves with mesh-sizes of 500  $\mu$ m and 100  $\mu$ m. Residues were dried, weighted again  
196 and then split on a dry micro-splitter. Where possible, at least 300 specimens of foraminifera  
197 were counted in every 5 cm of sediment. Species identification under a binocular microscope  
198 (Nikon SMZ1500) was supported using classification of Loeblich and Tappan (1987), with

199 few exceptions. Percentages of the 8 indicator species were applied. The number of species  
200 per sample and Shannon-Wiener Index were calculated in the program Primer 6. The benthic  
201 foraminiferal abundance and ice-rafted debris (IRD; grains >500  $\mu\text{m}$ ) were counted under a  
202 stereo-microscope and expressed as flux values (no. of specimens/grains  $\text{cm}^{-2} \text{ka}^{-1}$ ) using the  
203 bulk sediment density and sediment accumulation rate.

204 Stable oxygen and carbon isotope compositions of tests of the infaunal foraminifer species  
205 *Elphidium excavatum* f. *clavata* were determined at the Department of Geological Sciences,  
206 University of Florida (Florida, USA). All values are calibrated to the PeeDee Belemnite  
207 (PDB) scale and corrected for ice volume changes. In our study we discuss the  $\delta^{18}\text{O}$  and  $\delta^{13}\text{C}$   
208 record as a relative measure for changes in the water mass characteristics (temperature-  
209 salinity) and/or the supply of meltwater/freshwater to the area. Therefore, we haven't  
210 corrected the values for vital effect.

211 Grain size (<2 mm) analyses were performed every 1 cm using a Malvern Mastersizer  
212 2000 laser particle analyser and presented as volume percent. To examine relative variability  
213 in the near-bottom currents the mean grain size distribution of the <63  $\mu\text{m}$  fraction was  
214 calculated, to avoid effect of ice-rafted coarse fraction. Mean grain size was calculated in the  
215 program GRADISTAT 8.0 by the geometric method of moments (Blott and Pye, 2001).

### 216 **3.1 Age control**

217

218 The chronology for this study is based on high-precision AMS  $^{14}\text{C}$  measurements of  
219 fragments from nine calcareous bivalve shells. Measurements were performed in the Poznań  
220 Radiocarbon Laboratory, which is equipped with the 1.5 SDH-Pelletron Model "Compact  
221 Carbon AMS" (Czernik and Goslar, 2001; Goslar et al., 2004). The surface layer of shells was  
222 scraped off to avoid contamination with younger carbonate encrustation. The AMS  $^{14}\text{C}$  dates  
223 were converted into calibrated ages using the calibration program CALIB 6.1 (Stuiver and  
224 Reimer, 1993; Stuiver et al., 2005) and the Marine13 calibration curve (Reimer et al., 2013).  
225 The difference  $\Delta R$  in reservoir age correction of the model ocean and region of Svalbard was  
226 reported by Mangerud et al. (2006) to be  $105 \pm 24$  or  $111 \pm 35$ ; we used the first value;  
227 calibrated ages are presented in Table 2. It should be noted that the reservoir age is based on  
228 few data points from western Spitsbergen, and the age may be different for the eastern coast.  
229 However, no data are available from the latter region.

230

## 231 **4 Results**

232

#### 233 **4.1 Modern hydrology**

234

235 In November 2009 the surface water at the coring site (upper ~27 m) had already cooled  
236 down (1.24 °C; Fig. 2a). However, its salinity was still low (34.24 ‰). Transformed AW was  
237 observed in the layer between 60 and 160 m. The lowermost part of water column shows  
238 gradual cooling reaching a minimum temperature of 0.76 °C near the bottom. The lack of  
239 BSW at the bottom indicates gradual water mixing during summer and fall. In August 2013,  
240 the surface waters had slightly lower salinity, but the temperature was ~5 °C higher than in  
241 November 2009 (Fig. 2b). TAW occupied the same depths as in 2009. However, an almost 50  
242 m thick layer of BSW was present close to the seafloor.

243

#### 244 **4.2 Age model**

245

246 The <sup>14</sup>C ages and calibrated ages are reported in Table 2. The calibration gives an age  
247 distribution, not a single value, so the 2-sigma range presented and Fig. 3 shows age  
248 probability distribution curves. Ages of samples generally increase with sediment depth  
249 except in the case of one sample: St 20A 39, which provided an older age than the sample  
250 below. That shell was most likely re-deposited and was thus not used for the age model.  
251 However, because all the samples used for dating were shell fragments, it must be taken into  
252 account that it is possible that more samples could be subjected to re-deposition, but on the  
253 basis of the available data this is not possible to confirm. The age model is based on assuming  
254 linear sediment accumulation rates between data points. The highest probability peaks from  
255 calibrated age ranges were used as input values for the model. For the lowermost and  
256 uppermost parts of the core, we adopted sediment accumulation rates for the neighbouring  
257 parts. It is common to observe the loss of the sediment surface layer during coring with heavy  
258 gravity cores. In the case of core JM09-020-GC it is likely that at least the top 40 cm of  
259 sediments were lost during coring. This conclusion is supported by analysis of a box corer  
260 collected prior to coring (Łącka et al., in prep.). The extrapolated age model for the sediment  
261 surface is, therefore, 1200 cal yr BP.

262

#### 263 **4.3 Sedimentological and geochemical parameters**

264



265 The core JM09-020-GC is 426 cm long and consists of four lithological units L1  
266 (bottom of the core to 370 cm; >13,450 cal yr BP), L2 (370 cm to 272 cm; ~13,450 cal yr BP  
267 to ~11,500 cal yr BP), L3 (272 cm to 113 cm; ~11,500 cal yr BP to ~3600 cal yr BP) and L4  
268 (113 cm to core top; ~3600 cal yr BP to ~ 1200 cal yr BP). The lithological log was created  
269 based on the X-radiographs, grain-size analysis data and foraminiferal flux (Fig. 4). Grains >2  
270 mm are referred to as “clasts” and are marked in the lithological logs as individual features.

271 Unit L1 consists of compacted massive dark grey (5Y 4/1) sandy mud with various  
272 amounts of clasts. Bioturbation and foraminifera were generally absent. However, one shell  
273 fragment was found at approx. 395 cm.

274 Unit L2 contains massive dark grey (5Y 4/1) sandy mud with some coarser material  
275 and generally lower amounts of clasts than unit L1. The mean grain size (<63  $\mu\text{m}$ ) ranged  
276 from 7-10  $\mu\text{m}$ . The highest IRD flux and Fe/Ca ratio for the entire core occur in this unit. The  
277 mass accumulation rate (MAR) is 0.043  $\text{g cm}^{-2} \text{yr}^{-1}$ . The first signs of bioturbation occur in  
278 this unit and the flux of foraminifera increases rapidly up to ~5700 individuals  $\text{cm}^{-2} \text{ka}^{-1}$  (Fig.  
279 4).

280 The unit L3 is composed of massive dark olive grey mud (5Y 3/2) and is characterized  
281 by decreasing MAR values (0.019  $\text{g cm}^{-2} \text{yr}^{-1}$  to 0.002  $\text{g cm}^{-2} \text{yr}^{-1}$ ), moderate sand content and  
282 clearly increasing mean grain size (<63  $\mu\text{m}$ ). IRD flux is low and the Fe/Ca ratio decreases  
283 gradually until c. 9200 cal yr BP and then remains low (between 3 and 4; Fig. 4) Continuous  
284 bioturbation and variable foraminiferal fluxes, with maxima in the intervals 9000-8000 cal yr  
285 BP and 6000-5500 cal yr BP, are observed.

286 The uppermost unit L4 is mostly composed of the same material as the underlying  
287 unit- massive dark olive grey mud (5Y 3/2). However, the sand content is occasionally higher.  
288 MAR increases to 0.024  $\text{g cm}^{-2} \text{yr}^{-1}$ . The mean grain size (<63  $\mu\text{m}$ ) through this interval is  
289 even higher than in L3 and reaches up to 15  $\mu\text{m}$  and Fe/Ca ratio is increasing. The  
290 bioturbation continues, numerous shell fragments are presented and foraminifera flux reaches  
291 high values throughout the entire unit.

#### 292 **4.4 Foraminiferal fauna**

293

294 A total of 54 calcareous and 6 agglutinated species were identified. The foraminiferal  
295 assemblages were dominated by calcareous fauna. Agglutinated species occurred only in 14  
296 sediment samples, and their abundance did not exceeded 4%. The only exception is the  
297 sample dated to c. 11,350 cal yr BP (262.5 cm depth) with 25% of agglutinated foraminiferal

298 fauna. However, in this sample the total foraminifera abundance was low (13 specimens g<sup>-1</sup>  
299 sediment). In general, species richness, number of agglutinated foraminifera, as well as rare  
300 and fragile species, increase towards the top of the core. Benthic foraminiferal fauna is  
301 dominated by *Elphidium excavatum* f. *clavata*, *Cassidulina reniforme*, *Nonionellina*  
302 *labradorica*, *Melonis barleeanum*, *Islandiella* spp. (*Islandiella norcrossi*/*Islandiella helenae*)  
303 and *Cibicides lobatulus*. Percentages of *E. excavatum* f. *clavata* show an inverse relationship  
304 to *C. reniforme* with the almost constant dominance of the latter species in the periods:  
305 ~12,450 cal yr BP to ~12,000 cal yr BP and ~ 9600 cal yr BP to ~2800 cal yr BP (Fig. 5).  
306 Planktonic foraminifera are represented by three species, *Neogloboquadrina pachyderma*  
307 (sinistral), *Neogloboquadrina pachyderma* (dextral) and *Turborotalita quinqueloba*.  
308 However, the two later species are very rare. In general, the abundance of planktonic fauna is  
309 low in the older parts of the core and slightly increases approx. 10,000 cal yr BP reaching  
310 maximum values c. 2000 cal yr BP (Fig. 6).

311 Based on the most significant changes in the foraminiferal species abundances, species  
312 diversity and  $\delta^{18}\text{O}$  and  $\delta^{13}\text{C}$  in *E. excavatum* f. *clavata* tests the core was divided into the four  
313 foraminiferal zones F1-F4: ~13,450 cal yr BP to 11,500 cal yr BP (F1); 11,500 cal yr BP to  
314 9200 cal yr BP (F2); 9200 cal yr BP to 3600 cal yr BP (F3); 3600 cal yr BP to 1200 cal yr BP  
315 (F4) (Fig. 5, Fig. 6). Zones correspond to lithological division: the age of unit F4 is the same  
316 as L4, units F3 and F2 correspond to L3 and unit F1 is linked to unit L2. In unit L4  
317 foraminifera are rare to absent.

318 Zone F1 is dominated by the opportunistic *E. excavatum* f. *clavata* and *C. reniforme*.  
319 The latter one dominates over *E. excavatum* f. *clavata* between 12,250 cal yr BP and 11,950 cal  
320 yr BP. High percentages of *C. lobatulus* (up to 57%) and *Astrononion gallowayi* (up to 2.5%)  
321 occur occasionally. Planktonic foraminifera flux was low at the beginning of this section  
322 (mean value of 9 specimens cm<sup>-2</sup> ka<sup>-1</sup>) and completely disappeared for almost 1500 years  
323 from approx. 11,500 cal yr BP (Fig. 6). Species richness as well as Shannon-Wiener index  
324 show, compared to the upper part of the core, low biodiversity (mean values of 8 and 1.26,  
325 respectively). Furthermore, maxima of  $\delta^{18}\text{O}$  and  $\delta^{13}\text{C}$  occur in this interval.

326 In zone F2 the contribution of *E. excavatum* f. *clavata* and *C. reniforme* is slightly  
327 lower, and *N. labradorica* becomes the most abundant species (Fig. 5). There is also an  
328 increase in *Islandiella* spp. percentage. Planktonic foraminifera appeared again c. 10,000 cal  
329 yr BP. Biodiversity significantly increased and  $\delta^{18}\text{O}$  reached its minimum value of 2.61 ‰ vs  
330 VPDB approx. 10,000 cal yr BP.

331 Zone F3 is characterized by the minimum mass accumulation rates of sediment and  
332 consequently, low temporal resolution. *C. reniforme* dominates over *E. excavatum* f. *clavata*  
333 throughout. *M. barleeaanum* has its maximum abundance in this zone, and *N. labradorica* is  
334 abundant in the lower parts of this zone, decreasing at approx. 7000 cal yr BP. *Islandiella* spp.  
335 increases upcore. Planktonic foraminifera occur in the entire zone, and the fluxes are higher  
336 than those of previous units (Fig. 6). Biodiversity remains high in this zone, and  $\delta^{18}\text{O}$  and  
337  $\delta^{13}\text{C}$  remain generally stable, however marked peaks occurred at approx. 6800 cal yr BP,  
338 6500 cal yr BP and 5700 cal yr BP, respectively.

339 A consistently high foraminiferal flux of up to  $\sim 4900$  no. of specimens  $\text{cm}^{-2} \text{ka}^{-1}$   
340 characterises zone F4. The fluxes of *Islandiella* spp. and *Buccella* spp. increase significantly  
341 and from 2850 cal yr BP *Islandiella* spp. dominated the assemblage with *E. excavatum*  
342 f. *clavata*. Additionally, the fluxes of *C. lobatulus* and *A. gallowayi* increase. However, their  
343 abundances are lower than those of zone F2. A maximum abundance of planktonic  
344 foraminifera occurs in this unit. Foraminifera biodiversity continues to increase towards the  
345 core top (up to 2.33; Fig. 6).  $\delta^{18}\text{O}$  and  $\delta^{13}\text{C}$  increase slightly, however, with numerous  
346 fluctuations.

347

## 348 **5 Discussion**

349 Based on the most pronounced changes in sedimentological and foraminiferal data as  
350 well as comparison to previous studies from adjacent areas, we have distinguished 5 units in  
351 the studied core: a sub-glacial unit ( $>13,450$  cal yr BP), glacier-proximal unit (13,450 cal yr  
352 BP to 11,500 cal yr BP), glaciomarine unit I (11,500 cal yr BP to 9200 cal yr BP),  
353 glaciomarine unit II (9200 cal yr BP to 3600 cal yr BP) and glaciomarine unit III (3600 to  
354 1200 cal yr BP).

### 355 **5.1 Sub-glacial unit ( $>13,450$ cal yr BP)**

356 The lowermost unit L1 (Fig. 4) was significantly coarser, compacted and devoid of  
357 foraminifera, which indicates its likely of sub-glacial origin. During the late Weichselian  
358 Glacial Maximum, Storfjorden and Storfjordrenna were covered by an ice stream draining the  
359 Svalbard-Barents Ice Sheet (SBIS; e.g., Ottesen et al., 2005). The SBIS deglaciation occurred  
360 as a response to sea-level rise and increased mean annual temperature (Siegert and  
361 Dowdeswell, 2002). Rasmussen et al. (2007) noted that the outer part of Storfjordrenna (389  
362 m depth; Fig. 1a) was deglaciated before 19,700 cal yr BP. The bivalve shell fragment from

363 395.5 cm in our core suggests that the centre part of Storfjordrenna was ice-free before  
364 ~13,950 cal yr BP. This indicates that the ~100 km long retreat of the grounding line from the  
365 shelf break to the central part of Storfjordrenna occurred in approx. 5700 years. The  
366 deglaciation of the inner Storfjorden basin occurred c.11,700 cal yr BP (Rasmussen and  
367 Thomsen, 2014), while the coasts of east Storfjorden islands, Barentsøya and Edgeøya, which  
368 are located over 100 km north from the coring site, occurred some 500 years later, i.e., 11,200  
369 cal yr BP (recalibrated after Landvik et al., 1995). Siegert and Dowdeswell (2002) noted that,  
370 during the Bølling-Allerød warming (c. 14,700-12,700 cal yr BP), some of the deeper  
371 bathymetric troughs (e.g., Bjørnøyrenna) had deglaciated first, forming large embayments of  
372 ice around them. Probably, Storfjordrenna was one of such embayments at that time. Our data  
373 is in agreement with ice stream retreat dynamics presented by Rütther et al. (2012) and refines  
374 the recent models of the Barents Sea deglaciation (e.g. Winsborrow et al., 2010; Hormes et  
375 al., 2013; Andreassen et al., 2014).

## 376 **5.2 Glacier-proximal unit (13,450 cal yr BP to 11,500 cal yr BP)**

377

378 The transition from a subglacial to the glaciomarine setting is observed as a distinct  
379 change in sediment colour, several peaks of IRD, decreased amount of clasts and the  
380 appearance of foraminifera. The sediment accumulation rate ( $0.043 \text{ g cm}^{-2} \text{ yr}^{-1}$ ) was in the  
381 same order of magnitude as modern proximal and central parts of west Spitsbergen fjords (see  
382 Szczuciński et al., 2009 for review). Textural and compositional analyses of L2 recorded  
383 bimodal grain-size distribution and low abundance of microfossils, suggesting that deposition  
384 during the deglaciation occurred from suspension settling from sediment-laden plumes and ice  
385 rafting (Lucchi et al., 2013; Witus et al., 2014). This unit in our core is limited to ~60 cm and  
386 is characterized by a lack of bioturbation in its lower part.

387 The high flux of IRD supported by the high Fe/Ca ratio and depleted  $\delta^{18}\text{O}$  values  
388 correlates well with the abundance of *C. lobatulus* and *A. gallowayi* (Fig. 4 and Fig. 5), two  
389 species connected with high energy environments (Østby and Nagy, 1982) indicating that the  
390 coring site was likely located proximal to one or several ice fronts during the time of  
391 deposition of this unit.

392 During an early phase of the deglaciation of Storfjorden, the East Spitsbergen Current  
393 was still not active, because the ice sheet grounded between Svalbardbanken and  
394 Storfjordbanken blocked the passage between eastern and western Svalbard (Rasmussen et al.,  
395 2007; Hormes et al., 2013). Thus, the first foraminiferal propagules (juvenile forms) were

396 transported by sea currents (Alve and Goldstein, 2003) from the south and west and settled on  
397 the seafloor that was exposed after the retreat of grounded ice. The proximal glaciomarine  
398 environment affected foraminiferal assemblages and resulted in low species richness,  
399 biodiversity and low foraminiferal abundance. Consequently, foraminifera assemblages  
400 became dominated by fauna typical for the glacier proximal settings: *E. excavatum* f. *clavata*,  
401 *C. reniforme* and *Islandiella* spp. (e.g., Vilks, 1981; Osterman and Nelson, 1989; Polyak and  
402 Mikhailov, 1996; Hald and Korsun, 1997). Dominance of *E. excavatum* f. *clavata* confirms  
403 the proximity to the ice sheet, decreased salinity and high water turbidity (e.g., Steinsund,  
404 1994; Korsun and Hald, 1998; Włodarska-Kowalczyk et al., 2013).

405 The upper part of unit L2 (c. 12,800-11,500 cal yr BP) spans the Younger Dryas (YD)  
406 stadial. Records of marine sediments from Nordic and Barents Sea (e.g., Rasmussen et al.,  
407 2007; Ślubowska-Woldengen et al., 2007, 2008; Zamelczyk et al., 2012; Groot et al., 2014),  
408 as well as  $\delta^{18}\text{O}$  records from Greenland ice cores (e.g., Dansgaard et al., 1993; Grootes et al.,  
409 1993; Mayewski et al., 1993; Alley, 2000) show that the YD was characterised by a rapid and  
410 short-term temperature decrease. This event was likely driven by weakened North Atlantic  
411 Meridional Overturning Circulation, a result of the Lake Agassiz outburst (e.g., Gildor and  
412 Tziperman, 2001; Jennings et al., 2006; Murton et al., 2010; Cronin et al., 2012) or interaction  
413 between the sea ice and thermohaline water circulation (Broecker, 2006), which led to a  
414 reduction of AW transport to the north and a dominance of fresher Arctic Water. Our data  
415 shows that heavier  $\delta^{18}\text{O}$  recorded e.g., 12,720 cal yr BP and 12,100 cal yr BP, correlate with  
416 reduced to absent IRD fluxes, while the peaks of lighter  $\delta^{18}\text{O}$ , e.g., 12,450 cal yr BP, 12,150  
417 cal yr BP and 11,780 cal yr BP, occurred synchronously with significant enhanced IRD fluxes  
418 (Fig. 7). Absence of IRD, occasionally for several decades, might reflect temporarily polar  
419 conditions (Dowdeswell et al., 1998; Gilbert, 2000) characterized by the formation of  
420 perennial pack ice in Storfjorden locking icebergs proximal to their calving fronts and  
421 preventing their movement over the coring site (Forwick and Vorren, 2009). On the other  
422 hand, warmer periods resulted in massive iceberg rafting and delivery of IRD to  
423 Storfjordrenna, thus reflecting more sub-polar conditions. Hydrological variability during  
424 Younger Dryas was previously noted in some circum-North Atlantic deep-water records  
425 (Bakke et al., 2009; Elmore and Wright, 2011 and references therein; Pearce et al., 2013).  
426 Moreover, oxygen stable isotopes record from an ice-core GISP2 shows some warmer spells  
427 during that time (Stuiver et al., 1995), which coincides with higher ice-rafting in  
428 Storfjordrenna (Fig. 7). Bakke et al. (2009) noted that the earlier part of YD was colder and  
429 more stable, whereas later part of this period was characterized by alternations between sea-

430 ice cover and influx of warmer, salty North Atlantic waters. Our record shows that during the  
431 late YD  $\delta^{18}\text{O}$  were slightly shifted towards lighter values. Temporal resolution of our record  
432 do not allow for more detailed comparison with available data, nevertheless it clearly indicate  
433 that the Younger Dryas was not uniformly cold and that at least some warmer spells occurred  
434 on eastern Svalbard.

435 We also conclude that the data on  $\delta^{18}\text{O}$  presented in Fig. 7 reflects temperature variations  
436 at the coring site according to the isotopically lighter ArW paleotemperature model (Duplessy  
437 et al., 2005). Another explanation of the heavier  $\delta^{18}\text{O}$  periods during the YD could be  
438 intermittent inflow of warmer AW. However, this is unlikely to cause the synchronous  
439 disappearance of IRD.

440

### 441 **5.3 Glaciomarine unit I (early Holocene; 11,500 cal yr BP to 9200 cal yr BP)**

442

443 During the early Holocene foraminiferal fauna, although low in abundance, was  
444 dominated by species related to the glaciomarine environment (*E. excavatum* and *C.*  
445 *reniforme*; Fig. 5). Increasing species richness and biodiversity of foraminifera point to  
446 amelioration of environmental conditions and a progressive increase in the distance to the  
447 glacier front (Korsun and Hald, 2000; Włodarska-Kowalczyk et al., 2013). Decrease of the  
448 Fe/Ca ratio is suggested to reflect increased marine productivity and reduced supply of  
449 terrigenous material (Croudace et al., 2006). The mean grain size ( $>63\ \mu\text{m}$ ; Fig. 4) indicates  
450 weaker bottom currents at the beginning of the early Holocene and stronger bottom currents at  
451 the end of this period, which might have been related to the ongoing isostatic uplift of the land  
452 masses of Svalbard, as well as sea level rise (e.g., Forman et al., 2004).

453 Significant fluctuations of the  $\delta^{18}\text{O}$  and  $\delta^{13}\text{C}$  and increasing abundance of *N.*  
454 *labradorica* and *Islandiella* spp. suggest that Storfjordrenna was under the influence of  
455 various water masses at this time (Fig. 6). Comparison of our  $\delta^{18}\text{O}$  record with records from  
456 the Storfjorden shelf (400 m depth; Rasmussen et al., 2007; Fig. 1a) and the northern shelf of  
457 Svalbard (400 m depth; Ślubowska et al., 2005; Fig. 1b) show that all the records are shifted  
458 towards lighter values in the early Holocene (Fig. 8a) with the record from our core being the  
459 most depleted (from c. 13,000 cal yr BP). We suggest that the records located on the western  
460 and northern shelf of Svalbard directly mirror the effect of warmer Atlantic water inflow,  
461 while record from Storfjordrenna is under influence of isotopically lighter Arctic Water from  
462 the Barents Sea (Duplessy et al., 2005). The shift from the Arctic water domain to the Atlantic  
463 water domain during the end of the early Holocene is also visible on a scatter plot of  $\delta^{13}\text{C}$

464 against  $\delta^{18}\text{O}$  (Fig. 8b). The results grouped to the left indicate Arctic water domination, while  
465 the results grouped to the right shows Atlantic water domination.

466 According to Kaufman et al. (2004), the early Holocene is characterized by higher  
467 summer solar insolation at 60°N (10% higher than today), leading to a reduction in sea-ice  
468 cover (Sarnthein et al., 2003). As ice cover decreased, more solar energy was stored in  
469 summer and then re-radiated during the winter (e.g., Gildor and Tziperman, 2001). This  
470 process accelerated the ice sheet melting and finally, its retreat towards the fjord heads  
471 (Forwick & Vorren, 2009; Jessen et al., 2010; Baeten et al., 2010). Our data suggest that the  
472 iceberg calving to Storfjordrenna was significantly reduced or even disappeared approx.  
473 10,800 cal yr BP. However, supply of turbid meltwater from land to the study area still  
474 resulted in relatively high sediment accumulation rate.

475 According to Risebrobakken et al., (2011) and Groot et al., (2014) the presence of  
476 Arctic water suppressed the warming signal in the western Barents Sea. This is in agreement  
477 with our data on planktonic foraminifera reappearing at the termination of the early Holocene  
478 (c. 9600 cal yr BP; Fig.6). During this period *N. pachyderma* (sin.) dominated, however some  
479 peaks of *N. pachyderma* (dex.) and *T. quinqueloba* were noted. The two latter species are  
480 regarded as subpolar species (Bé and Tolderlund, 1971), although *T. quinqueloba* could be  
481 also related to oceanic frontal conditions separating Atlantic and Arctic water (Johannessen et  
482 al., 1994; Matthiessen et al., 2001). The peaks of *T. quinqueloba* around 9600 cal yr BP were  
483 noted previously in western Barents Sea margin (e.g. Hald et al., 2007; Risebrobakken et al.,  
484 2010).

485 Increasing foraminiferal biodiversity in Storfjordrenna (Fig. 6), as well as the  
486 occurrence of the thermophilous mollusc *Mytilus edulis* on western Edgeøya (Salvigsen et al.,  
487 1992) suggest that the inflow of AW crossed Storfjordrenna and continued northward to the  
488 inner fjord by 9600 cal yr BP.

489

#### 490 **5.4 Glaciomarine unit II (mid-Holocene; 9200 cal yr BP to 3600 cal yr BP)**

491

492 The mid-Holocene was characterized by relative stable environmental conditions, low  
493 sediment accumulation rates ( $0.002 \text{ g cm}^{-2}\text{yr}^{-1}$ ) and slight delivery of IRD (Fig. 4), reflecting  
494 very limited ice rafting and reduced supply of fine-grained material to Storfjordrenna. Low  
495 sedimentation rates and the low Fe/Ca ratio reflect reduced glacial conditions on Svalbard  
496 during the mid-Holocene (Elverhøi et al., 1995; Svendsen and Mangerud, 1997). In contrast,  
497 Hald et al. (2004) noted that in the record from Van Mijenfjorden, an enhanced tidewater

498 glaciation occurred during this period; it was thus argued that IRD is a more reliable indicator  
499 of glaciation than sedimentation rates. However, ice rafting in Storfjordrenna was generally  
500 low.

501 Shifts between the dominant species *C. reniforme* and *E. excavatum* f. *clavata* (Fig. 5)  
502 reflect environmental/hydrological changes (Hald and Korsun, 1997). The decrease of *E.*  
503 *excavatum* f. *clavata* (percentage and flux), which prefers colder bottom waters (Sejrup et al.,  
504 2004; Saher et al., 2009) and increase of *C. reniforme* points to the constant inflow of less  
505 modified AW and reduction in sedimentation (e.g., Schröder-Adams et al., 1990; Bergsten,  
506 1994; Jennings and Helgadóttir, 1994; Hald and Steinsund, 1996; Hald and Korsun, 1997).  
507 Furthermore, the relative abundance of *M. barleeianum* (Fig. 5) indicates that environmental  
508 conditions in Storfjordrenna were similar to contemporary Norwegian fjords that are  
509 dominated by AW with a temperature of 6 - 8 °C and salinities of 34 - 35 (Husum and Hald,  
510 2004). High total foraminiferal flux at the beginning of this period, as well as high  
511 foraminiferal species richness and biodiversity clearly point to AW conditions at the bottom  
512 (Hald and Korsun, 1997; Majewski and Zajączkowski, 2007; Włodarska-Kowalczyk et al.,  
513 2013). These conclusions are also supported by the heavier  $\delta^{18}\text{O}$ , showing AW dominance  
514 and significant reduction in the amount of freshwater and ArW in Storfjordrenna (Fig. 8). The  
515 continuous presence of *Mytilus edulis* during the entire mid-Holocene points to the reduced  
516 inflow of the East Spitsbergen Current on account of the AW inflow (Feyling-Hansen, 1955;  
517 Forman, 1990; Salvigsen et al., 1992. The pathway and range of AW inflow to the western  
518 and north-eastern Svalbard during mid-Holocene were well described by Ślubowska-  
519 Woldengen et al. (2008) and Groot et al. (2014). Together with our results it is suggested that  
520 one of the main ways of AW inflow to the eastern Svalbard may have occurred through  
521 Storfjordrenna.

522 Even though sediment accumulation rates were low, and grain size, as well as  
523 geochemical proxies, remain relatively constant during the mid-Holocene, the foraminiferal  
524 flux (including planktonic foraminifera) increased in two periods: of 9000 - 8000 cal yr BP  
525 and 6000 - 5500 cal yr BP, respectively (Fig. 4 and 6). In both cases the increase in IRD and *I.*  
526 *norcrossi* fluxes was followed by a slight depletion in  $\delta^{18}\text{O}$  and heavier  $\delta^{13}\text{C}$  suggesting minor  
527 cooling and likely seasonal sea-ice formation leading to beach sediment transport by shore  
528 ice. Our observations support earlier studies of the overall mid-Holocene shifts towards colder  
529 environment (Skirbekk et al., 2010; Rasmussen et al., 2012; Berben et al., 2014; Groot et al.,  
530 2014) and fluctuations in the glacial activity in the Svalbard region (e.g., Forwick and Vorren,  
531 2007, 2009; Beaten et al., 2010; Ojala et al., 2014). Our data shows an increased supply of



532 IRD fraction to Storfjordrenna sediment followed by variation of  $\delta^{18}\text{O}$ , however, high flux of  
533 *M. barleeanum* associated with Atlantic-derived waters (Steinsund, 1994; Jennings et al.,  
534 2004; Fig. 5) indicates AW condition in southern Storfjorden throughout the whole mid-  
535 Holocene. The similar ameliorated condition with consistent AW inflow prevailed over the  
536 mid-Holocene also in the Kveithola Trough south of Storfjordrenna (Berben et al., 2014;  
537 Groot et al., 2014). To a small extent these two signals (AW inflow and higher IRD flux) are  
538 not necessarily in contradiction, since snow accumulation on land and inconsiderable glaciers  
539 advance depend on humid air transport from the ocean. Thus slight change in the atmospheric  
540 frontal zone over Svalbard could cause fluctuation of the glaciers range.

541

### 542 **5.5 Glaciomarine unit III (late Holocene; 3600 cal yr BP to 1200 cal yr BP)**

543

544 The late Holocene is characterized by a gradual increase in sediment accumulation rates  
545 followed by numerous sharp peaks of sand content and minor peaks of IRD flux, as well as  
546 increased Fe/Ca ratio, indicating ice growth on land (compare with e.g. Svendsen and  
547 Mangerud, 1997; Hald et al., 2004; Forwick and Vorren, 2009; Kempf et al., 2013), slightly  
548 enhanced iceberg calving and/or ice rafting over the core site. The IRD record shows few  
549 irregular small peaks in the late Holocene (Fig. 7), which, according to Hass (2002), could be  
550 correlated with enhanced sea currents increasing the drift of the icebergs. Forwick et al.  
551 (2010) suggested several glacier front fluctuations during the past two millennia in  
552 Sassenfjorden and Tempelfjorden (W Spitsbergen), hence we suppose increased iceberg  
553 calving occurred at Storfjordrenna during this time. However, increased IRD flux can also  
554 reflect deposition related to enhanced shore ice rafting. The latter explanation is in agreement  
555 with heavier  $\delta^{18}\text{O}$  record (Fig. 6) indicating a minor cooling.

556 The mean grain size ( $<63\mu\text{m}$ ) increases in late Holocene (Fig. 4) and may indicate  
557 stronger bottom current velocities and winnowing of fine grained sediments. Andrleit et al.  
558 (2006) observed similar increased erosive activity of bottom currents during late Holocene on  
559 the SW Svalbard shelf. This sudden increase in current velocities may be connected with (1)  
560 postglacial reorganization of oceanographic conditions, (2) relative lowering of the sea level  
561 during the postglacial isostatic rebound and/or (3) more intensive sea-ice formation enhancing  
562 formation of BSW, forming seasonal near-bottom dense water mass flowing over the coring  
563 site (Andrleit et al., 1996). Nevertheless, this process is still not fully understood.

564 The sharp increase in the foraminiferal flux (Fig. 4) pointing to the increased nutrient  
565 advection/upwelling and biological productivity at the coring site during the late Holocene

566 was probably caused by variable hydrological conditions and most likely strong gradients  
567 leading to the formation of hydrological fronts. Our data shows increased fluxes of  
568 opportunistic species *E. excavatum* and *C. reniforme* as well as *N. labradorica* and *Islandiella*  
569 spp. *N. labradorica* and *Islandiella* spp. are abundant in areas with a high biological  
570 productivity in the upper surface waters (e.g. Hald and Steinsund, 1996; Korsun and Hald,  
571 2000; Knudsen et al., 2012). Abundant, though variable *M. barleeaanum*, documented in  
572 organic-rich mud within troughs of the Barents Sea (Hald and Steinsund, 1996) and in  
573 temperate fjords of Norway (Husum and Hald, 2004) points to high productivity in the  
574 euphotic zone leading to enhanced export of organic material/nutrients to the sea floor. Our  
575 data also shows high *N. pachyderma* flux throughout this unit, reflecting a significant increase  
576 of euphotic productivity at the coring site. However, low percentage of dextral specimens and  
577 *T. quinqueloba* point to low sea-surface temperatures (Fig. 6). This is in agreement with  
578 Rasmussen et al. (2014), who noted that after c. 3700 cal yr BP, Atlantic Water was only  
579 sporadically present at the surface. Cooling at the sea surface reflects the general trend in the  
580 Northern Hemisphere related to orbital forcing and reduction of summer insolation at high  
581 latitudes over the late Holocene (Wanner et al., 2008).

582 The last evidence of AW inflow to Edgøya area based on *M. edulis* is dated to 5000 cal yr  
583 BP (Hjort et al., 1995). After that time *M. edulis* remained absent until present days. However,  
584 its disappearance can rather be related to the freshening of surface water (Berge et al., 2006)  
585 and sea ice forcing as opposed to the extinction of AW in Storfjorden over the late Holocene  
586 (Rasmussen et al., 2007).

587

## 588 **6 Conclusions**

589

590 Multi-proxy analyses of one sediment core provide new information about the  
591 environmental development of the central part of Storfjordrenna off southern Svalbard since  
592 the late Bølling-Allerød. The main conclusions of our study are:

593 - Central Storfjordrenna was deglaciated before ~13,950 cal yr BP. The new data may help  
594 refine the future models of Svalbard-Barents Ice Sheet deglaciation.

595 - Between c. 13,450 to 11,500 cal yr BP, Storfjordrenna remained under the influence of  
596 Arctic Water masses with periodical sea-ice cover limiting the drift of icebergs. Nevertheless,  
597 at least three peaks of temperature increase during Younger Dryas stadial (12,800-11,500 cal

598 yr BP) presumably led to seasonal disappearance of sea ice and significantly enhanced IRD  
599 flux indicating more sub-polar conditions.

600 - Atlantic Water started to flow onto the shelves off Svalbard and into Storfjorden during the  
601 early Holocene leading to a progressive warming and significant glacial melting. From c.  
602 9600 cal yr BP, the Atlantic Water dominated the water column in Storfjordrenna.

603 - Environmental conditions off eastern Svalbard remained relatively stable from 9200-3600  
604 cal yr BP with glaciers smaller than those of today. However, some small-scale cooling events  
605 (9000 - 8000 cal yr BP and 6000 - 5500 cal yr BP) indicate minor fluctuations in  
606 climate/oceanography of Storfjordrenna.

607 - A surface-water cooling and freshening occurred in Storfjordrenna during the late Holocene,  
608 synchronously with glacier growth and cooling on land. Even though, AW was still present in  
609 the deeper part of Storfjordrenna. The late Holocene in Storfjordrenna has been characterized  
610 also by increased bottom currents velocities however the driving mechanism is not fully  
611 understood.

612  
613 *Acknowledgements.* The study was supported by the Institute of Oceanology Polish Academy  
614 of Science and the Polish Ministry of Science and Higher Education with grant no. NN 306  
615 469938. The <sup>14</sup>C dating was funded by Polish Ministry of Science and Higher Education grant  
616 No. IP2010 040970. We thank the captain and crew of R/V Jan Mayen, as well as the cruise  
617 participants, in particular Steinar Iversen, for their help at sea. Trine Dahl and Ingvild Hald  
618 are acknowledged for the acquisition of X-radiographs. Tine Rasmussen (UiT) is gratefully  
619 acknowledged for sharing the data with us. Katarzyna Zamelczyk (UiT) and Maria  
620 Włodarska-Kowalczyk (IOPAS) are thanked for help in planktonic foraminifera (Katarzyna)  
621 and bivalves (Maria) determination. Patrycja Jernas (UiT) helped during subsampling of the  
622 cores. Master's students from the University of Gdansk Kamila Sobala and Anna Nowicka  
623 helped with the Mastersizer2000 analysis. We are highly grateful Renata Lucchi (Istituto  
624 Nazionale di Oceanografia e Geofisica Sperimentale, Italy), Reignheid Skogseth (University  
625 Centre in Svalbard) and Ilona Goszczko (IOPAS) for the comments on the early version of  
626 this manuscript. We are sincerely indebted to Amy Lusher (Galway-Mayo Institute of  
627 Technology), Sara Strey-Mellema (University of Illinois) and Christof Pearce (Stockholm  
628 University) for improving the English of this manuscript. The comments from two  
629 anonymous referees helped to improve the manuscript considerably.

630 **References**

- 631 Aagaard, K., Foldvik, A. and Hillman, S.: The West Spitsbergen Current: disposition and  
632 water mass transformation, *J. Geophys. Res.*, 92, 3778-3784, 1987.
- 633 Akimova, A., Schauer, U., Danilov, S. and Núñez-Riboni, I.: The role of the deep mixing in  
634 the Storfjorden shelf water plume, *Deep Sea Res. I*, 58, 403-414, 2011.
- 635 Alley, R.: The Younger Dryas cold interval as viewed from central Greenland, *Quaternary*  
636 *Sci. Rev.*, 19 (1-5), 213-226, 2000.
- 637 Alley, R.B. and Augustdottir, A.M.: The 8 k event: cause and consequences of a major  
638 Holocene abrupt climate change, *Quaternary Sci. Rev.*, 24, 1123-1149, 2005.
- 639 Alve, E. and Goldstein, S.T.: Dispersal, survival and delayed growth of benthic foraminiferal  
640 propagules, *J. Sea Res.*, 63(1), 36- 51, 2010.
- 641 Andreassen, K., Winsborrow, M., Bjarnadóttir, L.R. and Rüther, D.C.: Ice stream retreat  
642 dynamics inferred from an assemblage of landforms in the northern Barents Sea, *Quat. Sci.*  
643 *Rev.*, doi: 10.1016/j.quascirev.2013.09.015, 2014.
- 644 Andruleit, H., Freiwald, A. and Schäfer, P.: Bioclastic carbonate sediments on the  
645 southwestern Svalbard shelf, *Mar. Geol.*, 134, 163–182, 1996.
- 646 Baeten, N.J., Forwick, M., Vogt, C. and Vorren, T.O.: Late Weichselian and Holocene  
647 sedimentary environments and glacial activity in Billefjorden, Svalbard, In: Howe, J.A.,  
648 Austin, W.E.N, Forwick, M. and Paetzel, M. (Editors): *Fjord Systems and Archives*, *Geol.*  
649 *Soc. London Spec. Publ.*, 344, 207-223, 2010.
- 650 Bakke, J., Lie, Ø., Heegaard, E., Dokken, T., Haug, G.H., Birks, H.H., Dulski, P. and Nilsen,  
651 T.: Rapid oceanic and atmospheric changes during the Younger Dryas cold period, *Nat.*  
652 *Geosci.*, 2, 202-205, 2009.
- 653 Bé, A.W.H. and D.S. Tolderlund: Distribution and ecology of living planktonic foraminifera  
654 in surface waters of the Atlantic and Indian oceans, in *The Micropaleontology of Oceans*,  
655 edited by B. M. Funnell and W. R. Riedel, pp. 105–149, Cambridge Univ. Press, Cambridge,  
656 U. K., 1971.
- 657 Berge, J., Johnsen, G., Nilsen, F., Gulliksen, B., Slagstad, D. and Pampanin, D.M.: The  
658 *Mytilus edulis* population in Svalbard: how and why, *Mar. Ecol. Prog. Ser.*, 309, 305-306,  
659 2006.
- 660 Bergsten, H.: Recent benthic foraminifera of a transect from the North Pole to the Yermak  
661 Plateau, eastern central Arctic Ocean, *Mar. Geol.*, 119 (3-4), 251-267, 1994.

662 Blott, S.J. and Pye, K.: GRADISTAT: a grain size distribution and statistics package for the  
663 analysis of unconsolidated sediments, *Earth Surf. Process. Landf.*, 26, 1237-1248, 2001.

664 Briner, J.P., Bini, A.C., and Anderson, R.S.: Rapid early Holocene retreat of a Laurentide  
665 outlet glacier through an Arctic fjord, *Nature Geosci.*, 2, 496-499, 2009.

666 Broecker, W.S.: Was the Younger Dryas triggered by a flood? *Science*, 312, 1146–1148, doi:  
667 10.1126/science.1123253, 2006.

668 Cronin, T.M., Rayburn, J.A., Guilbault, J.-P., Thunell, R. and Franzi, D.A.: Stable isotope  
669 evidence for glacial lake drainage through the St.Lawrence Estuary, eastern Canada, ~13.1-  
670 12.9 ka, *Quat. Sci. Rev.*, 260, 55-65, 2012.

671 Croudace, I. W., Rindby, A. and Rothwell, R. G.: ITRAX: description and evaluation of a  
672 new multi-function X-ray core scanner, *Geol. Soc. London, Spec. Publ.*, 267, 51–63, 2006.

673 Czernik, J. and Goslar, T.: Preparation of graphite targets in the Gliwice Radiocarbon  
674 Laboratory for AMS <sup>14</sup>C dating, *Radiocarbon*, 43, 283–291, 2001.

675 Dansgaard, W., Johnsen, S.J., Clausen, H.B., Dahl-Jensen, D., Gundestrup, N.S., Hammer, C.  
676 U.C., Hvidberg, S., Steffensen, J.P., Sveinbjörnsdottir, A. E., Jouzel, J. and Bond G.:  
677 Evidence for general instability of past climate from a 250-kyr ice-core record, *Nature*, 364,  
678 218 – 220, doi:10.1038/364218a0, 1993.

679 Dowdeswell, J.A., Elverhøi, A. and Spielhagen, R.: Glacimarine sedimentary processes and  
680 facies on the polar north Atlantic margins, *Quat. Sci. Rev.*, 17, 243–272, 1998.

681 Duplessy, J.C., Cortijo, E., Ivanova, E., Khusid, T., Labeyrie, L., Levitan, M., Murdmaa, I.  
682 and Paterne, M.: Paleoceanography of the Barents Sea during the Holocene,  
683 *Paleoceanography*, 20(4), PA4004, doi: 10.1029/2004PA001116, 2005.

684 Dylmer, C.V., Giraudeau, J., Eynaud, F., Husum, K. and de Vernal, A.: Northward advection  
685 of Atlantic water in the eastern Nordic Seas over the last 3000 yr, *Clim. Past*, 9, 1505-1518,  
686 2013.

687 Elmore, A.C. and Wright, J.D: North Atlantic Deep Water and climate variability during the  
688 Younger Dryas cold period, *Geology*, 39:107, 2011.

689 Elverhøi, A., Svendsen, J.I., Solheim, A., Andersen, E.S., Milliman, J., Mangerud, J. and  
690 Hooke, R.L.: Late Quaternary Sediment Yield from the High Arctic Svalbard Area, *J. Geol.*,  
691 103, 1-17, 1995.

692 Fer, I., Skogseth, R., Haugan, P.M. and Jaccard, P.: Observations of the Storfjorden  
693 overflow, *Deep-Sea Res. I*, 50(10-11), 1283-1303, doi: 10.1016/S0967-0637(03)00124-9,  
694 2003.

695 Fer, I., Skogseth, R. and Haugan, P.M.: Mixing of the Storfjorden overflow (Svalbard  
696 Archipelago) inferred from density overturns, *J. Geophys. Res.*, 109,  
697 C01005, doi:10.1029/2003JC001968, 2004.

698 Feyling-Hanssen, R. and Jørstad, F.: Quaternary fossil from the Sassen-area in Isfjorden,  
699 west-Spitsbergen (the marine mollusk fauna), *Norsk Polarinstitutt Skrifter*, 94, 1-85, 1950.

700 Feyling-Hanssen, R.: Stratigraphy of the marine late-Pleistocene of Billefjorden,  
701 Vestspitsbergen, *Norsk Polarinstitutt Skrifter*, 107, 1-186, 1955.

702 Forman, S.L.: Post-glacial relative sea level history of northwestern Spitsbergen, Svalbard, B.  
703 *Geol. Soc. of America*, 102, 1580–1590, 1990.

704 Forman, S.L., Lubinski, D.J., Ingólfsson, Ó., Zeeberg, J.J., Snyder, J.A., Siegert, M.J. and  
705 Matishov, G.G.: A review of postglacial emergence on Svalbard, Franz Josef Land and  
706 Novaya Zemlya, northern Eurasia, *Quaternary Sci. Rev.*, 23, 1391-1434, 2004.

707 Forwick, M. and Vorren, T.O.: Holocene mass-transport activity in and climate outer  
708 Isfjorden, Spitsbergen: marine and subsurface evidence, *The Holocene*, 17(6), 707-716, 2007.

709 Forwick, M. and Vorren, T.O.: Late Weichselian and Holocene sedimentary environments  
710 and ice rafting in Isfjorden, Spitsbergen, *Palaeogeogr., Palaeoclim., Palaeoecol.*, 280, 258-  
711 274, 2009.

712 Forwick, M., Vorren, T.O., Hald, M., Korsun, S., Roh, Y., Vogt, C. and Yoo, K.-C.: Spatial  
713 and temporal influence of glaciers and rivers on the sedimentary environment in  
714 Sassenfjorden and Tempelfjorden, Spitsbergen. In: Howe, J.A., Austin, W.E.N, Forwick, M.  
715 and Paetzel, M. (Editors): *Fjord Systems and Archives*, *Geol. Soc. London, Spec. Pub.*, 344,  
716 163-193, 2010.

717 Gammelsrod, T. and Rudels, B.: Hydrographic and current measurements in the Fram Strait,  
718 *Pol. Res.*, 1, 115-126, 1983.

719 Geyer, F., Fer, I. and Smedsrud, L.: Structure and forcing of the overflow at the Storfjorden  
720 sill and its connection to the Arctic coastal polynya in Storfjorden, *Ocean Sci. Disc.*, 7, 17-49,  
721 2010.

722 Gilbert, R.: Environmental assessment from the sedimentary record of highlatitude fiords,  
723 *Geomorphology*, 32, 295–314, 2000.

724 Gildor, H. and Tziperman, E.: A sea ice climate switch mechanism for the 100-kyr glacial  
725 cycles, *J. Geophys. Res.*, 106, 9117-9133, 2001.

726 Goslar, T., Czernik, J. and Goslar, E.: Low-energy <sup>14</sup>C AMS in Poznań Radiocarbon  
727 Laboratory, Poland, *Nucl. Instrum. Methods*, B 223/224, 5–11, 2004.

728 Groot, D.E., Aagaard-Sørensen, S. and Husum, K.: Reconstruction of Atlantic water  
729 variability during the Holocene in the western Barents Sea, *Clim. Past*, 10, 51-62, 2014.

730 Grootes, P. M., Stuiver, M., White, J. W. C., Johnsen, S. J. and Jouzel, J.: Comparison of  
731 oxygen isotope records from the GISP2 and GRIP Greenland ice cores, *Nature*, London, 366,  
732 552-554, 1993.

733 Haarpaintner, J., Gascard, J. and Haugan, P.M.: Ice production and brine formation in  
734 Storfjorden, Svalbard, *J. Geophys. Res.*, 106, doi: 10.1029/1999JC000133, 2001.

735 Hald, M., Ebbsen, H., Forwick, M., Godtlielsen, F., Khomenko, L., Korsun, S., Olsen, L.R.  
736 and Vorren, T.O.: Holocene paleoceanography and glacial history of the West Spitsbergen  
737 area, Euro-Arctic margin, *Quaternary Sci. Rev.*, 23, 2075-2088, 2004.

738 Hald, M. and Korsun, S.: Distribution of modern Arctic benthic foraminifera from fjords of  
739 Svalbard, *J. Foramin. Res.*, 27, 101-122, 1997.

740 Hald, M. and Steinsund, P.I.: Benthic foraminifera and carbonate dissolution in surface  
741 sediments of the Barents-and Kara Seas, In: Stein, R., Ivanov, G.I., Levitan, M.A. and Fahl,  
742 K. (Editors), *Surface-sediment composition and sedimentary processes in the central Arctic  
743 Ocean and along the Eurasian Continental Margin*, *Ber. Polarforsch.*, 212, 285-307, 1996.

744 Hald, M., Andersson, C., Ebbesen, H., Jansen, E., Klitgaard-Kristensen, D., Risebrobakken,  
745 B., Salomonsen, G.R., Sarnthein, M., Sejrup, H.P. and Telford, R.J.: Variations in  
746 temperature and extent of Atlantic Water in the Northern North Atlantic during the Holocene,  
747 *Quat. Sci. Rev.*, 26, 3423–40, 2007.

748 Hald, M. and Korsun, S.: The 8200 cal. yr BP event reflected in the Arctic fjord, Van  
749 Mijenfjorden, Svalbard, *The Holocene*, 18, 981 – 990, doi: 10.1177/0959683608093536,  
750 2008.

751 Hansen, J., Hanken, N., Nielsen, J., Nielsen, J. and Thomsen, E.: Late Pleistocene and  
752 Holocene distribution of *Mytilus edulis* in the Barents Sea region and its paleoclimatic  
753 implications, *J. Biogeogr.*, 38, 1197-1212, 2011.

754 Hass, H. C.: A method to reduce the influence of ice-rafted debris on a grain size record from  
755 northern Fram Strait, *Polar Res.*, 21(2), 299-306, 2002.

756 Hjort, C., Andrielson, L., Bondevik, S., Landvik, J., Mangerud, J. and Salvigsen, O.: *Mytilus*  
757 *edulis* on eastern Svalbard- dating the Holocene Atlantic Water influx maximum, *Lundqua*  
758 *Rep.*, 35, 171-175, 1992.

759 Hjort, C., Mangerud, J., Andrielson, L., Bondevik, S., Landvik, J. Y. and Salvigsen, O.:  
760 Radiocarbon dated common mussels *Mytilus edulis* from eastern Svalbard and the Holocene  
761 marine climatic optimum, *Polar Res.*, 14(2), 239–243, 1995.

762 Hormes, A., Gjermundsen, E.F. and Rasmussen, T.L.: From mountain top to the deep sea -  
763 deglaciation in 4D of the northwestern Barents Sea, *Quaternary Sci. Rev.*, 75, 78-99, 2013.

764 Husum, K. and Hald, M.: A continuous marine record 8000-1600 cal. yr BP from the  
765 Malangenfjord, north Norway: foraminiferal and isotopic evidence, *The Holocene*, 14, 877 –  
766 887, 2004.

767 Jennings, A.E., Knudsen, K.L., Hald, M., Hansen, C.V. and Andrews, J.T.: A mid-Holocene  
768 shift in Arctic sea-ice variability on the East Greenland Shelf, *The Holocene*, 12 (1), 49-58,  
769 2002.

770 Jennings, A.E. and Helgadottir, G.: Foraminiferal assemblages from the fjords and shelf of  
771 Eastern Greenland, *J. Foramin. Res.*, 24, 123–44, 1994.

772 Jennings, A.E., Hald, M., Smith, M., and Andrews, J.T.: Freshwater forcing from the  
773 Greenland Ice Sheet during the Younger Dryas: evidence from southeastern Greenland shelf  
774 cores, *Quaternary Sci. Rev.*, 25, 282-298, 2004.

775 Jennings, A.E., Hald, M., Smith, M., and Andrews, J.T.: Freshwater forcing from the  
776 Greenland Ice Sheet during the Younger Dryas: evidence from southeastern Greenland shelf  
777 cores, *Quat. Sci. Rev.*, 25, 282-298, 2006.

778 Jessen, S.P., Rasmussen, T.L., Nielsen, T. and Solheim, A.: A New Late Weichselian And  
779 Holocene Marine Chronology For The Western Svalbard Slope 30,000 - 0 Cal Years BP,  
780 *Quaternary Sci. Rev.*, 29 (9-10), 1301 – 1312, doi: 10.1016/j.quascirev.2010.02.020, 2010.

781 Johannessen, T., Jansen, E., Flatøy, A. and Ravelo, A.C.: The relationship between surface  
782 water masses, oceanographic fronts and paleoclimatic proxies in surface sediments of the  
783 Greenland, Iceland, Norwegian Seas, In Zahn, R., Kominski, M. and Labyrie, L., editors,  
784 *Carbon cycling in glacial ocean: constraints on the ocean's role in global change*. Springer-  
785 Verlag, 61–85, 1994.

786 Kaufman, D. S., Ager, T. A., Anderson, N. J., Anderson, P. M., Andrews, J. T., Bartlein, P. J.,  
787 Brubaker, L. B., Coats, L. L., Cwynar, L. C., Duvall, M. L., Dyke, A. S., Edwards, M. E.,  
788 Eisner, W. R., Gajewski, K., Geirsdóttir, A., Hu, F. S., Jennings, A. E., Kaplan, M. R.,  
789 Kerwin, M. W., Lozhkin, A. V., MacDonald, G. M., Miller, G. H., Mock, C. J., Oswald, W.  
790 W., Otto-Bliesner, B. L., Porinchu, D. F., Rühland, K., Smol, J. P., Steig, E. J. and Wolfe, B.  
791 B.: Holocene thermal maximum in the western Arctic (0-180°W), *Quaternary Sci. Rev.*, 23  
792 (5-6), 529 – 560, 2004.

793 Kempf, P., Forwick, M., Laberg, J.S. and Vorren, T.O.: Late Weichselian – Holocene  
794 sedimentary palaeoenvironment and glacial activity in the high-Arctic van Keulenfjorden,  
795 Spitsbergen, *The Holocene*, 23, 1605-1616, 2013.



796 Klitgaard Kristensen, D., Rasmussen T.L. and Koç, N.: Palaeoceanographic changes in the  
797 northern Barents Sea during the last 16 000 years- new constraints on the last deglaciation of  
798 the Svalbard-Barents Sea Ice Sheet, *Boreas*, 42, 798-813, 2013.

799 Knudsen, K. L., Eiríksson, J. and Bartels-Jónsdóttir, H. B.: Oceanographic changes through  
800 the last millennium off North Iceland: Temperature and salinity reconstructions based on  
801 foraminifera and stable isotopes, *Mar. Micropaleontol.*, 54–73, 2012.

802 Korsun, S. and Hald, M.: Modern benthic foraminifera off tide water glaciers, Novaja Semlja,  
803 Russian Arctic, *Arctic Alpine Res.*, 30 (1), 61-77, 1998.

804 Korsun, S. and Hald, M.: Seasonal dynamics of benthic foraminifera in a glacially fed fjord of  
805 Svalbard, European Arctic, *J. Foramin. Res.*, 30(4), 251-271, 2000.

806 Kubischta, F., Knudsen, K. L., Kaakinen, A. and Salonen, V.-P.: Late Quaternary  
807 foraminiferal record in Murchisonfjorden, Nordaustlandet, Svalbard, *Polar Res.*, 29, 283–297,  
808 2010.

809 Landvik, J.Y., Hjort, C., Mangerud, J., Möller, P. and Salvigsen, O.: The Quaternary record of  
810 eastern Svalbard: an overview, *Polar Res.*, 14, 95-103, 1995.

811 Lloyd, J.M., Park, L.A., Kuijpers, A., Moros, M.: Early Holocene palaeoceanography and  
812 deglacial chronology of Disko Bugt, West Greenland, *Quaternary Sci. Rev.*, 24, 1741-1755,  
813 2005.

814 Loeblich, A.R. and Tappan, H.: *Foraminiferal Genera and Their Classification*, Van Nostrand  
815 Reinhold, New York, 970, 1987.

816 Loeng, H.: Features of the physical oceanographic conditions of the Barents Sea, *Polar Res.*,  
817 10, 5–18, 1991.

818 Lubinski, D. J., Forman, S. L. and Miller, G. H.: Holocene glacier and climate fluctuations on  
819 Franz Josef Land, Arctic Russia, 80°N, *Quaternary Sci. Rev.*, 18, 85-108, 1999.

820 Lucchi, R.G., Camerlenghi, A., Rebesco, M., Colmenero-Hidalgo, E., Sierro, F.J., Sagnotti,  
821 L., Urgeles, R., Melis, R., Morigi, C., Bárcena, M.-A., Giorgetti, G., Villa, G., Persico, D.,  
822 Flores, J.-A., Rigual-Hernández, A.S., Pedrosa, M.T., Macri, P. and Caburlotto, A.:  
823 Postglacial sedimentary processes on the Storfjorden and Kveithola trough mouth fans:  
824 Significance of extreme glacial sedimentation, *Global Planet. Change*, 111, 309-326, 2013.

825 Lydersen, C., Nøst, O., Lovell, P., McConell, B., Gammelsrød, T., Hunter, C., Fedak, M.,  
826 Kovacs, K.: Salinity and temperature structure of a freezing Arctic fjord- monitored by white  
827 whales (*Delphinapterus leucas*), *Geophys. Res. Lett.*, 29, doi: 10.1029/2002GL015462, 2002.

828 Majewski, W. and Zajączkowski, M.: Benthic foraminifera in Adventfjorden, Svalbard: Last  
829 50 years of local hydrographic changes, *J. Foramin. Res.*, 37, 107-124, 2007.

830 Mangerud, J., Bondevik, S., Gulliksen, S., Hufthammer, A.K. and Høisæter, T.: Marine <sup>14</sup>C  
831 reservoir ages for 19<sup>th</sup> century whales and molluscs from the North Atlantic, *Quaternary Sci.*  
832 *Rev.*, 25, 3228-3245, 2006.

833 Matthiessen, J., Baumann, K.H., Schröder-Ritzrau, A., Hass, C., Andrulleit, H., Baumann, A.,  
834 Jensen, S., Kohly, A., Pflaumann, U., Samtleben, C., Schäfer, P. and Thiede, J.: Distribution  
835 of calcareous, siliceous and organic-walled planktic microfossils in surface sediments of the  
836 Nordic seas and their relation to surface-water masses, In Schäfer, P., Ritzrau, W., Schlüter,  
837 M. and Thiede, J., editors, *The northern North Atlantic: a changing environment*. Springer,  
838 105–27, 2001.

839 Mayewski, P.A., Meeker, L.D., Morrison, M.C., Twickler, M.S., Whitlow, S.I., Ferland,  
840 K.K., Meese, D.A., Legrand, M.R. and Steffensen, J.P.: Greenland ice core “signal”  
841 characteristics: An expanded view of climate change, *J. Geophys. Res.*, 98, doi:  
842 10.1029/93JD01085, 1993.

843 McCarthy, D.J.: *Late Quaternary Ice-ocean Interactions in Central West Greenland*,  
844 Department of Geography, Durham University, Durham, UK, 2011.

845 Munsell® Color Geological Rock-Color Chart Revised Washable Edition, 2009.

846 Murton, J.B., Bateman, M.D., Dallimore, S.R., Teller, J.T. and Yang, Z.: Identification of  
847 Younger Dryas outburst flood path from Lake Agassiz to the Arctic Ocean, *Nature*, 464, 740-  
848 743, 2010.

849 Norges Sjøkartverk: *Den norske los- Arctic pilot*, Farvannbeskrivelse, sailing directions,  
850 Svalbard-Jan Mayen, Seventh edition, Stavanger, Norwegian Hydrographic Service,  
851 Norwegian Polar Institute, 1988.

852 O'Dwyer, J., Kasajima, Y., and Nøst, O.: North Atlantic water in the Barents Sea opening,  
853 1997 to 1999, *Polar Res.*, 2, 209–216, 2001.

854 Ojala, A.E. K., Salonen, V.-P., Moskalik, M., Kubischta, F. and Oinonen, M.: Holocene  
855 sedimentary environment of a High–Arctic fjord in Nordaustlandet, Svalbard, *Pol. Polar Res.*,  
856 03, 35(1), 73-98, 2014.

857 Østby, K. L. and Nagy, J.: Foraminiferal Distribution in the Western Barents Sea, Recent and  
858 Quaternary, *Polar Res.*, 1, 55–95, 1982.

859 Osterman, L.E. and Nelson, A.R.: Latest Quaternary and Holocene paleoceanography of the  
860 eastern Baffin Island continental shelf, Canada: benthic foraminiferal evidence, *Can. J. Earth*  
861 *Sci.*, 26(11), 2236-2248, 1989.

862 Ottesen, D., Dowdeswell J.A. and Rise, L.: Submarine landforms and the reconstruction of  
863 fast-flowing ice streams within a large Quaternary ice sheet: the 2500-km-long Norwegian–  
864 Svalbard margin (57°–80°N), *Geol. Soc. Am. Bull.*, 117, 1033–1050, 2005.

865 Pearce, C., Seidenkrantz, M.-S., Kuijpers, A., Massé, G., Reynisson, N.F. and Kristiansen,  
866 S.M.: Ocean lead at the termination of the Younger Dryas cold spell, *Nature Comm.*, 4, 1664,  
867 2013.

868 Pedrosa, M. T., Camerlenghi, A., de Mol, B., Urgeles, R., Rebesco, M., Lucchi, R. G.,  
869 Amblas, D., Calafat, A., Canals, M., Casamor, J. L., Costa, S., Frigola, J., Iglesias, O.,  
870 Lafuerza, S., Lastras, G., Lavoie, C., Liqueste, C., Hidalgo, E. C., Flores, J. A., Sierro, F. J.,  
871 Carburlotto, A., Grossi, M., Winsborrow, M., Zgur, F., Deponte, D., De Vittor, C., Facchin,  
872 L., Tomini, I., De Vittor, R., Pelos, C., Persissinotto, G., Ferrante, N. and Di Curzio, E.:  
873 Seabed morphology and shallow sedimentary structure of the Storfjorden and Kveithola  
874 trough-mouth fans northwest Barents Sea, *Mar. Geol.*, 286, 1-4, 2011.

875 Piechura, J.: Dense bottom waters in Storfjord and Storfjordrenna, *Oceanologia*, 38, 285-292,  
876 1996.

877 Polyak, L. and Mikhailov, V.: Post-glacial environments of the southeastern Barents Sea:  
878 Foraminiferal evidence, *Geol. Soc. London, Spec. Publ.*, 111, 323-337, 1996.

879 Polyak, L. and Solheim, A.: Late- and post-glacial environments in the northern Barents Sea  
880 west of Franz Josef Land, *Polar Res.*, 13, 97-207, 1994.

881 Quadfasel, D., Rudels, B., and Kurz, K.: Outflow of dense water from a Svalbard fjord into  
882 the Fram Strait, *Deep-Sea Res.*, 35, 1143-1150, 1988.

883 Quadfasel, D. A., Sy, A., Wells, D. and Tunik, A.: Warming in the Arctic, *Nature*, 350, 385,  
884 1991.

885 Rasmussen, T., L., Thomsen, E., Slubowska-Woldengen, M., Jessen, S., Solheim, A. and  
886 Koc, N.: Paleoceanographic evolution of the SW Svalbard margin (76°N) since 20,000 <sup>14</sup>C yr  
887 BP, *Quaternary Res.*, 67, 100-114, doi: 10.1016/j.yqres.2006.07.002, 2007.

888 Rasmussen, T.L. and Thomsen, E.: Stable isotope signals from brines in the Barents Sea:  
889 Implications for brine formation during the last glaciation, *Geology*, 37 (10), 903 – 906, doi:  
890 10.1130/G25543A.1, 2009.

891 Rasmussen, T.L., Forwick, M. and Mackensen, A.: Reconstruction of inflow of Atlantic  
892 Water to Isfjorden, Svalbard during the Holocene: Correlation to climate and seasonality,  
893 *Mar. Micropaleontol.*, 94-95, 80 – 90, doi: 10.1016/j.marmicro.2012.06.008, 2012.

894 Rasmussen, T.L., Thomsen, E., Skirbekk, K., Ślubowska-Woldengen, M., Klitgaard  
895 Kristensen, D., Koç, N.: Spatial and temporal distribution of Holocene temperature maxima in

896 the northern Nordic seas: interplay of Atlantic-, Arctic- and polar water masses, *Quaternary*  
897 *Sci. Rev.*, 92, 280-291, <http://dx.doi.org/10.1016/j.quascirev.2013.10.034>, 2014.

898 Rasmussen, T.L. and Thomsen, E.: Brine formation in relation to climate changes and ice  
899 retreat during the last 15,000 years in Storfjorden, Svalbard, 76–78°N, *Paleoceanography*, doi:  
900 10.1002/2014PA002643, 2014.

901 Rasmussen, T.L. and Thomsen, E.: Palaeoceanographic development in Storfjorden,  
902 Svalbard, during the deglaciation and Holocene: evidence from benthic foraminiferal records,  
903 *Boreas*, doi: 10.1111/bor.12098 (in press)

904 Reimer, P.J., Bard, E., Bayliss, A., Beck, J.W., Blackwell, P.G., Bronk Ramsey, C., Buck,  
905 C.E., Cheng, H., Edwards, R.L., Friedrich, M., Grootes, P.M., Guilderson, T.P., Haflidason,  
906 H., Hajdas, I., HattĀŠ, C., Heaton, T.J., Hogg, A.G., Hughen, K.A., Kaiser, K.F., Kromer, B.,  
907 Manning, S.W., Niu, M., Reimer, R.W., Richards, D.A., Scott, E.M., Southon, J.R., Turney,  
908 C.S.M., van der Plicht, J.: IntCal13 and MARINE13 radiocarbon age calibration curves 0-  
909 50000 years cal BP, *Radiocarbon* 55(4), 2013, doi: 10.2458/azu\_js\_rc.55.16947

910 Risebrobakken, B., Moros, M., Ivanova, E. V., Chistyakova, N., and Rosenberg, R.: Climate  
911 and oceanographic variability in the SW Barents Sea during the Holocene, *The Holocene*, 20,  
912 609–621, doi:10.1177/0959683609356586, 2010.

913 Risebrobakken, B., Dokken, T., Smedsrud, L., Andersson, C., Jansen, E., Moros, M., and  
914 Ivanova, E.: Early Holocene temperature variability in the Nordic Seas: The role of oceanic  
915 heat advection versus changes in orbital forcing, *Paleoceanography*, 26, PA4206,  
916 doi:10.1029/2011PA002117, 2011.

917 Rūther, D., Bjarnadóttir, L., R., Junttila, J., Husum, K., Rasmussen, T.L., Lucchi, R., G. and  
918 Andreassen, K.: Pattern and timing of the northwestern Barents Sea Ice Sheet deglaciation  
919 and indications of episodic Holocene deposition, *Boreas*, 41(3), 494-512, doi:10.1111/j.1502-  
920 3885.2011.00244.x, 2012.

921 Saher, M.H., Klitgaard Kristensen, D., Hald, M., Korsun, S. and Jørgensen, L.L.: Benthic  
922 foraminifera assemblages in the Central Barents Sea: an evaluation of the effect of combining  
923 live and total fauna studies in tracking environmental change, *Norw. J. Geol.*, 89, 149-161,  
924 2009.

925 Salvigsen, O., Forman S. and Miller, G.: Thermophilous mollusks on Svalbard during the  
926 Holocene and their paleoclimatic implications, *Polar Res.*, 11, 1-10, 1992.

927 Sarnthein, M., van Kreveld, S., Erlenkeuser, H., Grootes, P.M., Kucera, M., Pflaumann, U.  
928 and Sculz, M.: Centennial-to-millennial-scale periodicities of Holocene climate and sediment  
929 injections off the western Barents shelf, 75°N, *Boreas*, 32, 447-461, 2003.

930 Schauer, U.: The release of brine-enriched shelf water from Storfjord into the Norwegian Sea,  
931 *J. Geophys. Res.-Oceans*, 100, 60515-16028, 1995.

932 Schauer, U. and Fahrbach, E.: A dense bottom water plume in the western Barents Sea:  
933 Downstream modification and interannual variability, *Deep-Sea Res. I*, 46, 2095-2108, 1999.

934 Schauer, U., Fahrbach, E., Østerhus, S. and Rohardt, G.: Arctic Warming through the Fram  
935 Strait: Oceanic heat transport from 3 years of measurements, *J. Geophys. Res.*, 109, C06026,  
936 2004.

937 Schröder-Adams, C.J., Cole, F.E., Medioli, F.S., Mudie, P.J., Scott, D.B., and Dobbin, L.:  
938 Recent Arctic shelf foraminifera: Seasonally ice covered areas vs. perennially ice covered  
939 areas, *J. Foramin. Res.*, 20(1), 8 – 36, 1990.

940 Sejrup, H.P., Birks, H.J.B., Kristensen, D.K. and Madsen, H.: Benthonic foraminiferal  
941 distributions and quantitative transfer functions for the northwest European continental  
942 margin. *Mar. Micropaleontolog.*, 53 (1-2), 197 – 226, 10.1016/j.marmicro.2004.05.009, 2004.

943 Serreze, M. C., Maslanik, J. A., Scambos, T. A., Fetterer, F., Stroeve, J., Knowles, K.,  
944 Fowler, C., Drobot, S., Barry R. G. and Haran., T. M.: A new record minimum Arctic sea ice  
945 and extent in 2002, *Geophys. Res. Lett.*, 30, 1110, doi:10.1029/2002GL016406, 2003.

946 Siegert, M.J. and Dowdeswell, J.A.: Late Weichselian iceberg, surface-melt and sediment  
947 production from the Eurasian Ice Sheet: results from numerical ice sheet modeling, *Mar.*  
948 *Geol.*, 188, 109-127, 2002.

949 Skirbekk, K., Klitgaard Kristensen, D., Rasmussen, T., Koç, N. and Forwick, M.: Holocene  
950 climate variations at the entrance to a warm Arctic fjord: evidence from Kongsfjorden  
951 Trough, Svalbard, In: Howe, J.A., Austin, W.E.N, Forwick, M. and Paetzel, M.  
952 (Editors): *Fjord Systems and Archives*, *Geol. Soc. London, Spec. Publ.*, 344, 289-304, 2010.

953 Skogseth, R., Haugan, P. M. and Haarpaintner, J.: Ice and brine production in Storfjorden  
954 from four winters of satellite and in situ observations and modeling, *J. Geophys. Res.*, 109  
955 (C10), doi: 10.1029/2004JC002384, 2004.

956 Skogseth, R., Haugan, P. M. and Jakobsson, M.: Watermass transformations in Storfjorden,  
957 *Cont. Shelf Res.*, 25, 667–695, 2005.

958 Ślubowska, M.A., Koç, N., Rasmussen, T.L. and Klitgaard-Kristensen, D.: Changes in the  
959 flow of Atlantic water into the Arctic Ocean since the last deglaciation: Evidence from the  
960 northern Svalbard continental margin, 80°N, *Paleoceanography*, 20, 1-16, doi:  
961 10.1029/2005PA001141, 2005.

962 Ślubowska-Woldengen, M., Rasmussen, T.L., Koç, N., Klitgaard-Kristensen, D., Nilsen, F.  
963 and Solheim, A.: Advection of Atlantic Water to the western and northern Svalbard shelf

964 since 17,500 cal yr BP, *Quaternary Sci. Rev.*, 26, 463-478, doi:  
965 10.1016/j.quascirev.2006.09.009, 2007.

966 Ślubowska-Woldengen, M., Koç, N., Rasmussen, T.L., Klitgaard-Kristensen, D., Hald, M.  
967 and Jennings, A.E.: Time-slice reconstructions of ocean circulation changes on the continental  
968 shelf in the Nordic and Barents Seas during the last 16,000 cal yr B.P., *Quaternary Sci. Rev.*,  
969 27, 1476 – 1492, doi: 10.1016/j.quascirev.2008.04.015, 2008.

970 Smedsrud, L. H., Esau, I., Ingvaldsen, R. B., Eldevik, T., Haugan, P. M. and co-authors: The  
971 role of the Barents Sea in the Arctic climate system, *Rev. Geophys.*, 51, 415-449, 2013.

972 Spielhagen, R.F., Werner, K., Sørensen, S.A., Zamelczyk, K., Kandiano, E., Budéus, G.,  
973 Husum, K., Marchitto, T.M., Hald, M.: Enhanced Modern Heat Transfer to the Arctic by  
974 Warm Atlantic Water, *Science*, 331 (6016), 450 – 453, doi: 10.1126/science.1197397, 2011.

975 Steinsund, P.I.: Benthic foraminifera in surface sediments of the Barents and Kara seas:  
976 modern and late Quaternary applications, PhD thesis, University of Tromsø, 1994.

977 Stuiver, M., Grootes, P.M., Braziunas, T.F.: The GISP2 <sup>18</sup>O climate record of the past 16,500  
978 years and the role of the sun, ocean and volcanoes, *Quaternary Res.*, 44, 341-354, 1995.

979 Stuiver, M. and Reimer, P. J.: Extended <sup>14</sup>C database and revised CALIB radiocarbon  
980 calibration program, *Radiocarbon*, 35, 215–230, 1993.

981 Stuiver, M., Reimer, P. J., and Reimer, R. W.: CALIB 5.0. [WWW program and  
982 documentation], 2005.

983 Svendsen, J. I., Elverhøi, A. and Mangerud, J.: The retreat of the Barents Sea Ice Sheet on the  
984 western Svalbard margin, *Boreas*, 25, 244-256, 1996.

985 Svendsen, J. I. and Mangerud, J.: Holocene glacial and climatic variations on Spitsbergen,  
986 Svalbard, *The Holocene*, 7, 45-57, 1997.

987 Svendsen, H., Beszczynska-Møller, A., Hagen, J.O., Lefauconnier, B., Tverberg, V., Gerland,  
988 S., Ørebæk J.B., Bischof, K., Papucci, C., Zajączkowski, M., Azzolini, R., Bruland, O.,  
989 Wiemcke, C., Winther, J.-G. and Dallmann, W.: The physical environment of Kongsfjorden-  
990 Krossfjorden, an Arctic fjord system in Svalbard, *Polar Res.*, 21, 1, 133-166, 2002.

991 Szczuciński, W., Zajączkowski, M., Scholten, J.: Sediment accumulation rates in subpolar  
992 fjords - impact of post-Little Ice Age glaciers retreat, Billefjorden, Svalbard, *Estuarine Coast.*  
993 *Shelf Sci.*, 85, 345-356, 2009.

994 Thorarinsdóttir, G. and Gunnarson, K.: Reproductive cycles of *Mytilus edulis* L. on the west  
995 and east coast of Iceland, *Polar Res.*, 22, 217-223, 2003.

996 Vilks, G.: Late glacial-postglacial foraminiferal boundary in sediments of eastern Canada,  
997 Denmark and Norway, *Geosci. Canada*, 8, 48-55, 1981.

998 Walczowski, W. and Piechura, J.: New evidence of warming propagating toward the Arctic  
999 Ocean, *Geophys. Res. Lett.*, 33, L12601, doi:10.1029/2006GL025872, 2006.

1000 Walczowski, W. and Piechura, J.: Pathways of the Greenland Sea warming, *Geophys. Res.*  
1001 *Lett.*, 34, L10608, doi:10.1029/2007GL029974, 2007.

1002 Walczowski, W., Piechura, J., Goszczko, I. and Wieczorek, P.: Changes in Atlantic water  
1003 properties: an important factor in the European Arctic marine climate, *ICES J. Mar. Sci.*,  
1004 69(5), 864–869, doi:10.1093/icesjms/fss068, 2012.

1005 Wanner, H., Beer, J., Bütikofer, J., Crowley, T.J., Cubasch, U., Flückiger, J., Goosse, H.,  
1006 Grosjean, M., Joos, F., Kaplan, J.O., Küttel, M., Müller, S., Prentice, I.C., Solomina, O.,  
1007 Stocker, T.F., Tarasov, P., Wagner, M. and Widmann, M.: Mid- to late Holocene climate  
1008 change: an overview, *Quaternary Sci. Rev.*, 27, 1791-1828, 2008.

1009 Weber, M.E., Niessen, F., Kuhn, G. and Wiedicke-Hombach, M.: Calibration and application  
1010 of marine sedimentary physical properties using a multi-sensor core logger, *Mar. Geol.*,  
1011 136(3-4), 151-172, doi:10.1016/S0025-3227(96)00071-0, 1997.

1012 Werner, K., Spielhagen, R. F., Bauch, D., Hass, H. C., Kandiano, E. S. and Zamelczyk, K.:  
1013 Atlantic Water advection to the eastern Fram Strait - multiproxy evidence for late Holocene  
1014 variability, *Palaeogeogr., Palaeoclim., Palaeoecol.*, 308(3-4), 264-276, 2011.

1015 Winkelmann, D. and Knies, J.: Recent distribution and accumulation of organic carbon on the  
1016 continental margin west off Spitsbergen, *Geochem., Geophys., Geosyst.*, 6(9), Q09012,  
1017 doi:10.1029/2005GC000916, 2005.

1018 Winsborrow, M.C.M., Andreassen, K., Corner, G.D. and Laberg, J.S.: Deglaciation of a  
1019 marine-based ice sheet: Late Weichselian Palaeo-ice dynamics and retreat in the southern  
1020 Barents Sea reconstructed from onshore and offshore glacial geomorphology, *Quat. Sci. Rev.*  
1021 29 (3e4), 424e442, 2010.

1022 Witus, A.E., Braneky, C.M., Anderson, J.B., Szczuciński, W., Schroeder, D.D. and  
1023 Jakobsson, M.: Meltwater intensive glacial retreat in polar environments and investigation of  
1024 associated sediments: example from Pine Island Bay, West Antarctica, *Quat. Sci. Rev.*, 85,  
1025 99-118, 2014.

1026 Włodarska-Kowalczyk, M., Pawłowska, J. and Zajączkowski, M.: Do foraminifera mirror  
1027 diversity and distribution patterns of macrobenthic fauna in an Arctic glacial fjord? *Mar.*  
1028 *Micropaleontol.*, 103, 30-39, 2013.

1029 Zajączkowski, M., Szczuciński, W. and Bojanowski, R.: Recent sediment accumulation rates  
1030 in Adventfjorden, Svalbard, *Oceanologia*, 46, 217-231, 2004.

1031 Zajączkowski, M., Nygård, H., Hegseth, E.N., Berge, J.: Vertical flux of particulate matter in  
1032 an Arctic fjord: the case of lack of the sea-ice cover in Adventfjorden 2006 – 2007, *Polar*  
1033 *Biology*, 33, 223-239, 2010.

1034 Zamelczyk, K., Rasmussen, T.L., Husum, K., Haflidason, H., de Vernal, A., Ravna, E.K.,  
1035 Hald, M. and Hillaire-Marcel, C.: Paleoceanographic changes and calcium carbonate  
1036 dissolution in the central Fram Strait during the last 20 ka, *Quaternary Res.*, 78, 405-416,  
1037 2012.

1038

1039

1040

1041

1042

1043

1044

1045

1046

1047

1048

1049

1050

1051

1052

1053

1054

1055

1056

1057

1058

1059

1060

1061

1062

1063

1064



1065 **Table 1**

1066 Water mass characteristics in Storfjorden and Storfjordrenna (Skogseth et al., 2005,  
 1067 modified). The two main water masses are in bold.

Watermass names	Watermass characteristics	
	Temperature (°C)	Salinity
<b>Atlantic Water (AW)</b>	<b>&gt;3.0</b>	<b>&gt;34.95</b>
<b>Arctic Water (ArW)</b>	<b>&lt;0.0</b>	<b>34.3-34.8</b>
Brine-enriched Shelf Water (BSW)	<-1.5	>34.8
Surface Water (SW)	>0.0	<34.4
Transformed Atlantic Water (TAW)	>0.0	>34.8

1068

1069

1070

1071

1072

1073

1074

1075

1076

1077

1078

1079

1080

1081 **Table 2**1082 AMS <sup>14</sup>C dates and calibrated ages.

<i>Sample No</i>	<i>Depth [cm]</i>	<i>Lab No.</i>	<i>Raw AMS <sup>14</sup>C BP</i>	<i>Calibrated years BP ± 2σ</i>	<i>Cal yr BP used in age model</i>	<i>Dated material</i>
St 20A 5/6	5	Poz-46955	1835 ± 30 BP	1200 – 1365	1285	<i>Cilliatocardium cilliatum</i>
St 20A 39	38.5	Poz-46957	2755 ± 30 BP	2245 – 2470	Not used	<i>Astarte crenata</i>
St 20 78/79	78	Poz-46958	2735 ± 30 BP	2177 – 2429	2320	<i>Astarte crenata</i>
St 20 110	109.5	Poz-46959	3450 ± 30 BP	3079 – 3323	3220	<i>Astarte crenata</i>
St 20 142	141.5	Poz-46961	6580 ± 40 BP	6850 – 7133	6970	<i>Astarte crenata</i>
St 20A 152	151.5	Poz-46962	7790 ± 40 BP	8018 – 8277	8160	<i>Astarte crenata</i>
St 20 157	156.5	Poz-46963	8610 ± 50 BP	8989 – 9288	9120	<i>Batharca glacialis</i>
St 20 251/252/253	252	Poz-46964	10,200 ± 60 BP	10,895 – 11,223	11,230	<i>Thracia sp</i>
St 20 396	395.5	Poz-46965	12,570 ± 60 BP	13,780 – 14,114	13,950	Bivalvia shell

1083

1084

1085

1086

1087

1088

1089

1090

1091

1092

1093

1094

1095

1096

1097

1098

1099

1100

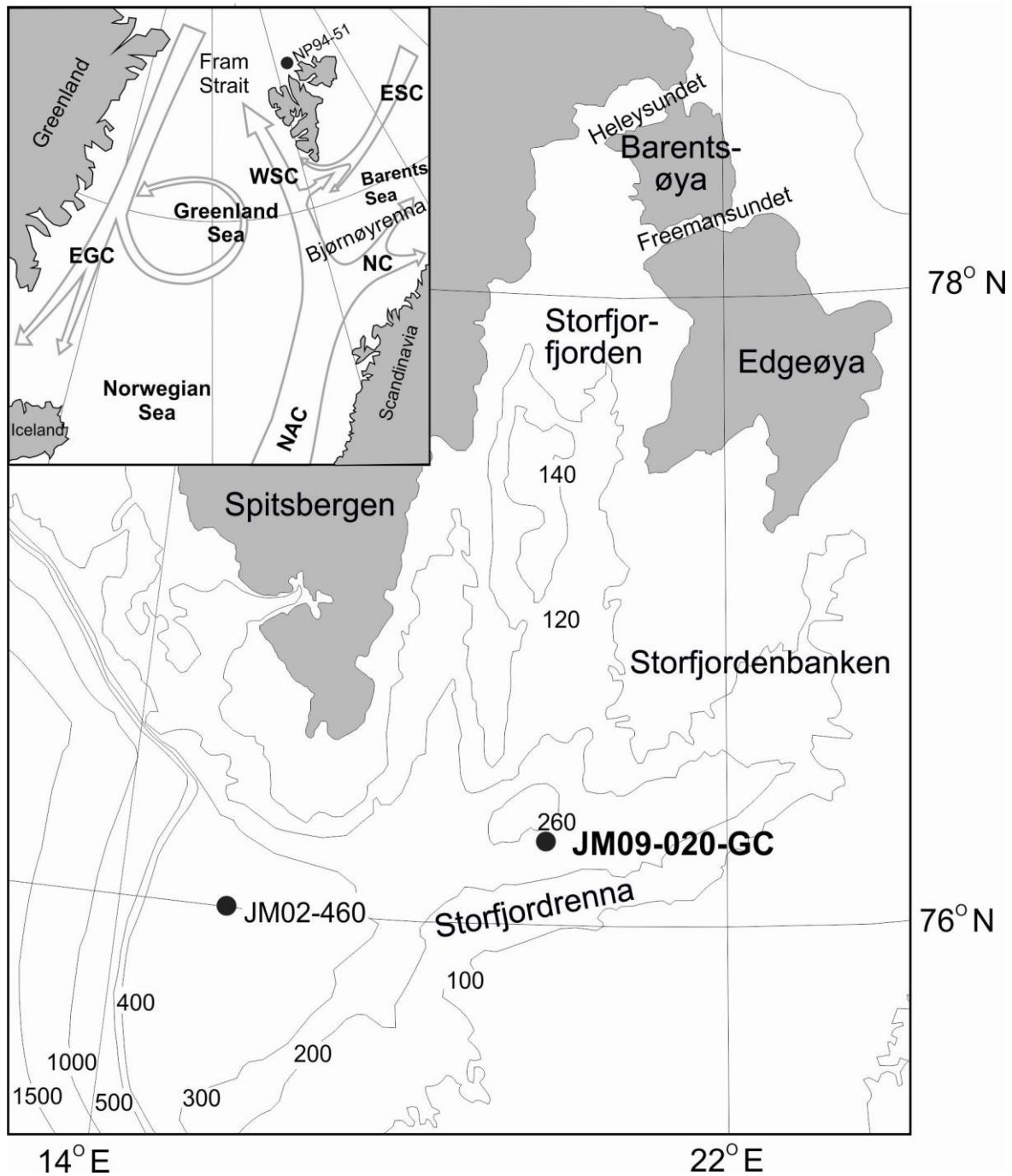
1101

1102

1103

1104

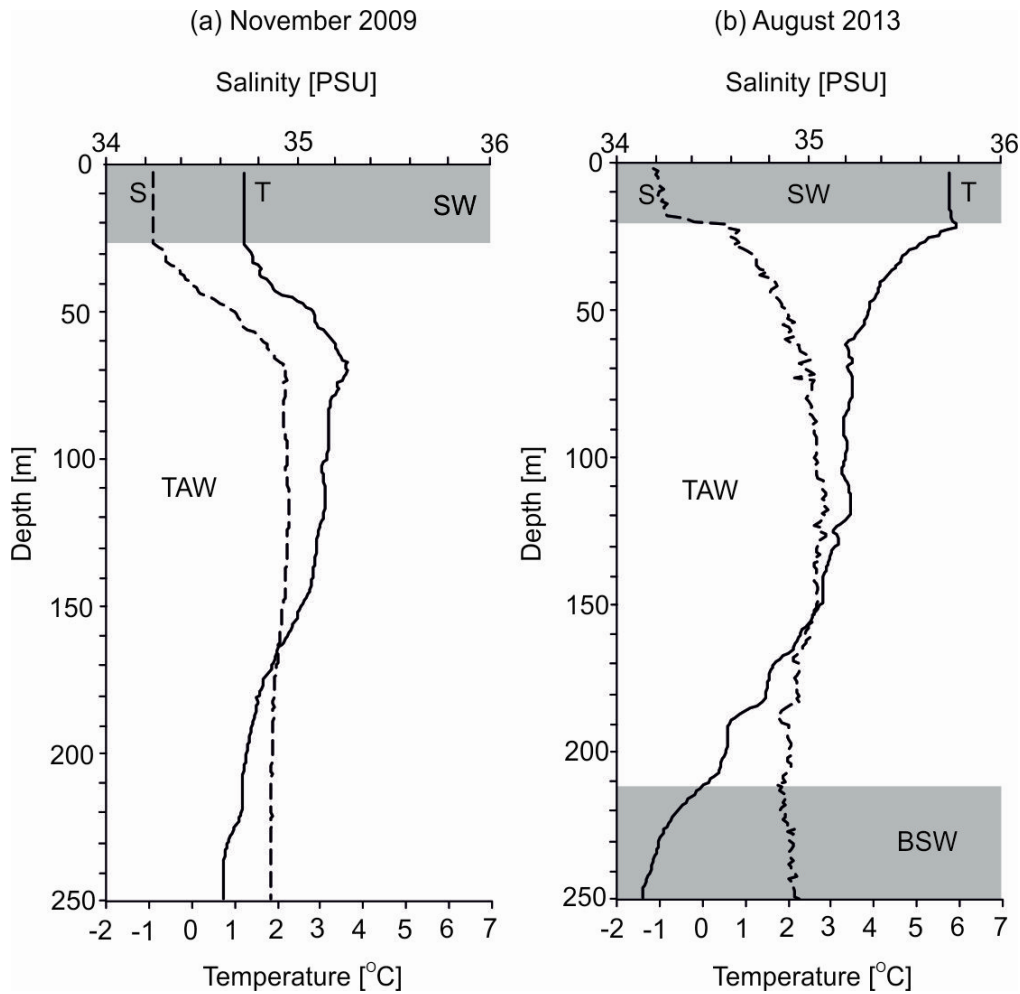
1105



1106  
1107

1108 Fig. 1. Location map (a) showing the core site from this study (JM09-020-GC) and core site  
1109 of JM02-460 (Rasmussen et al., 2007). The inlet map (b) shows the modern surface oceanic  
1110 circulation in Nordic Seas and location of a core NP94-51 (Ślubowska et al., 2005).  
1111 Abbreviations: NAC- Norwegian-Atlantic Current; WSC- West Spitsbergen Current; ESC-  
1112 East Spitsbergen Current; EGC- East Greenland Current; NC- Norwegian Current. The cores  
1113 JM02-460 and NP94-51 are discussed in the text.

1114



1115

1116

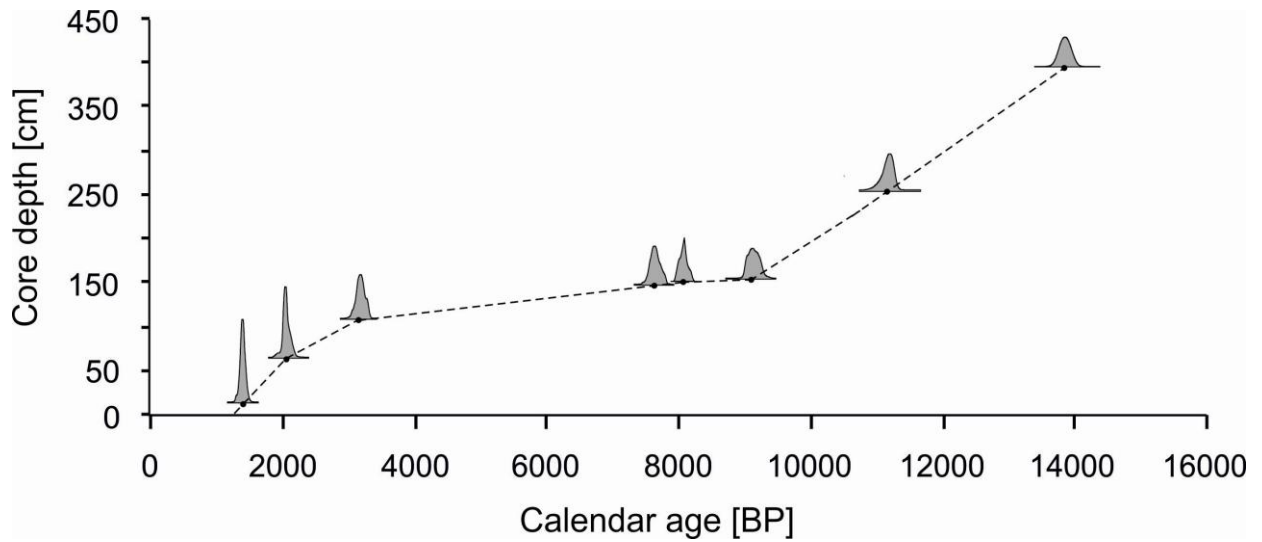
1117 Fig. 2. Temperature and salinity versus depth, measured in November 5<sup>th</sup> 2009 (a) and in

1118 August 13<sup>th</sup> 2013 (b) at the site of core JM09-020GC. SW - Surface Water, TAW -

1119 Transformed Atlantic Water, BSW - Brine-enriched Shelf Water.

1120

1121

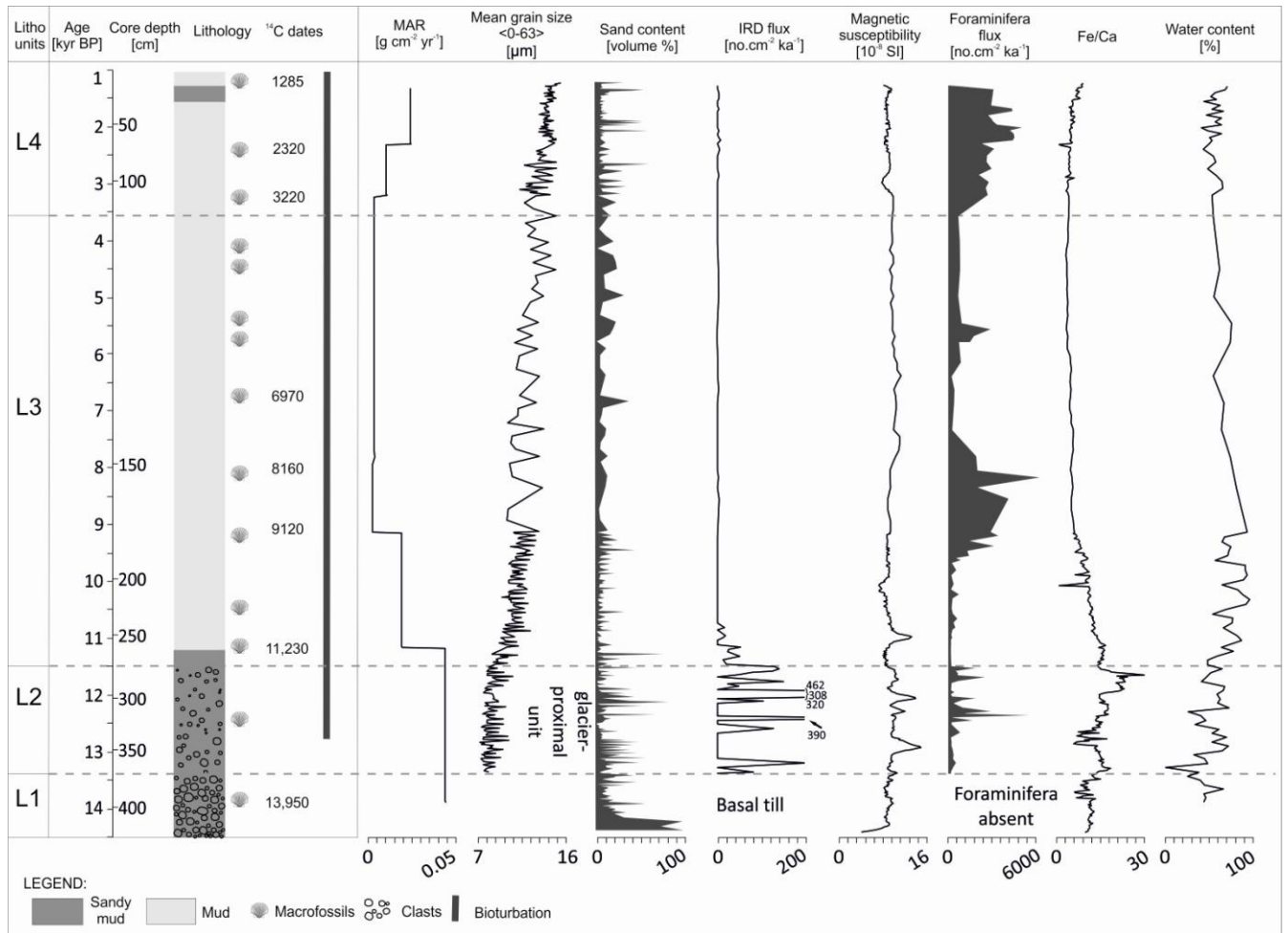


1122  
1123

1124 Fig. 3. Age-depth relationship for JM09-020-GC based on 8 AMS <sup>14</sup>C calibrated ages with 2-  
1125 sigma age probability distribution curves. The chronology is established by linear  
1126 interpolation between the calibrated ages.

1127

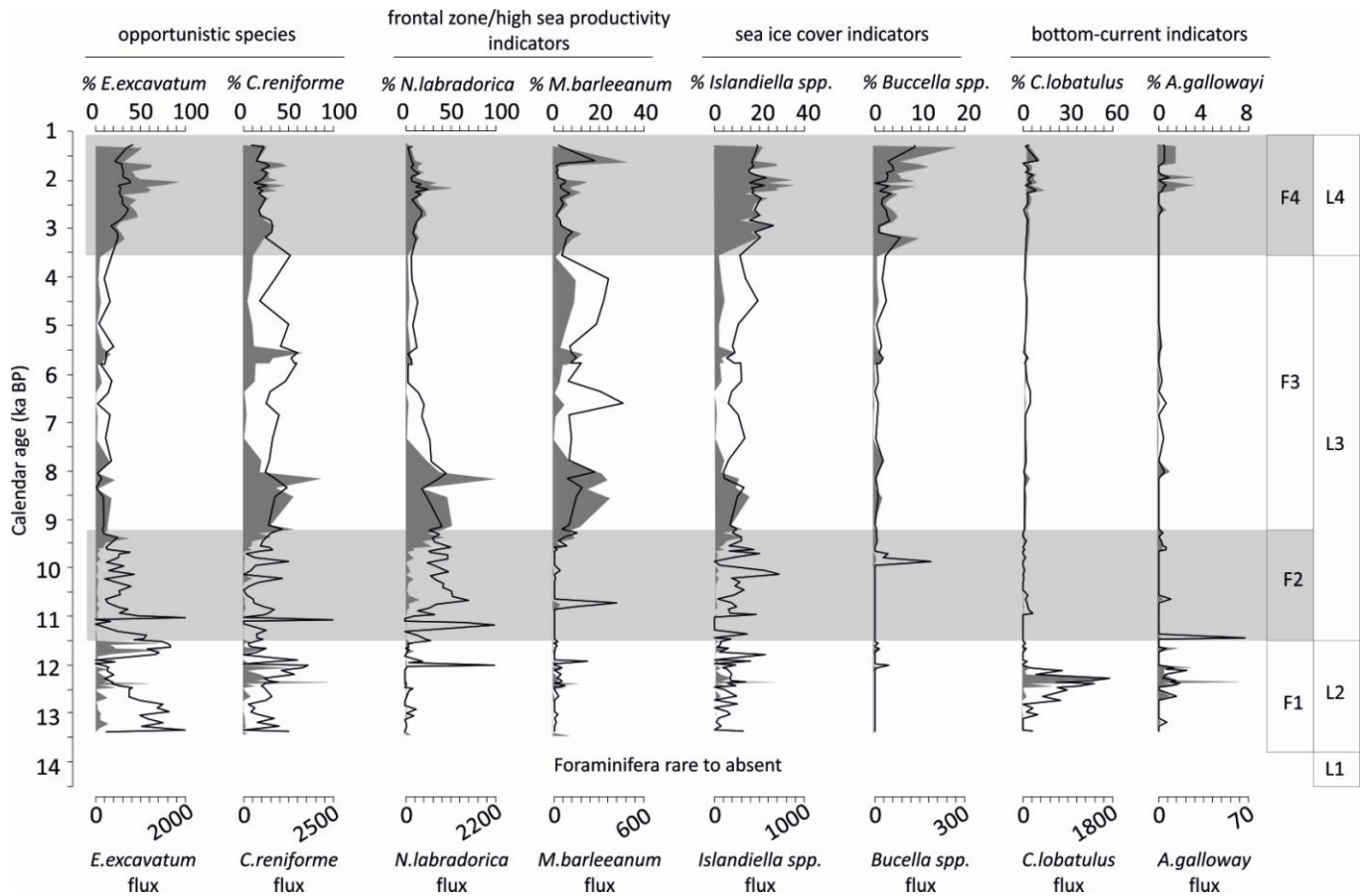
1128



1129  
1130

1131 Fig. 4. Lithological log of core JM09-020GC. Lithology, <sup>14</sup>C dates, occurrence of  
1132 bioturbation, mass-accumulation rates, mean grain size in the range of 0-63 μm, sand content,  
1133 ice-rafted debris flux, magnetic susceptibility, foraminifera flux as well as Fe/Ca ratio and  
1134 water content. The results are presented with lithostratigraphic units (L1-L4), versus calendar  
1135 years (cal kyr BP) and core depth (cm).

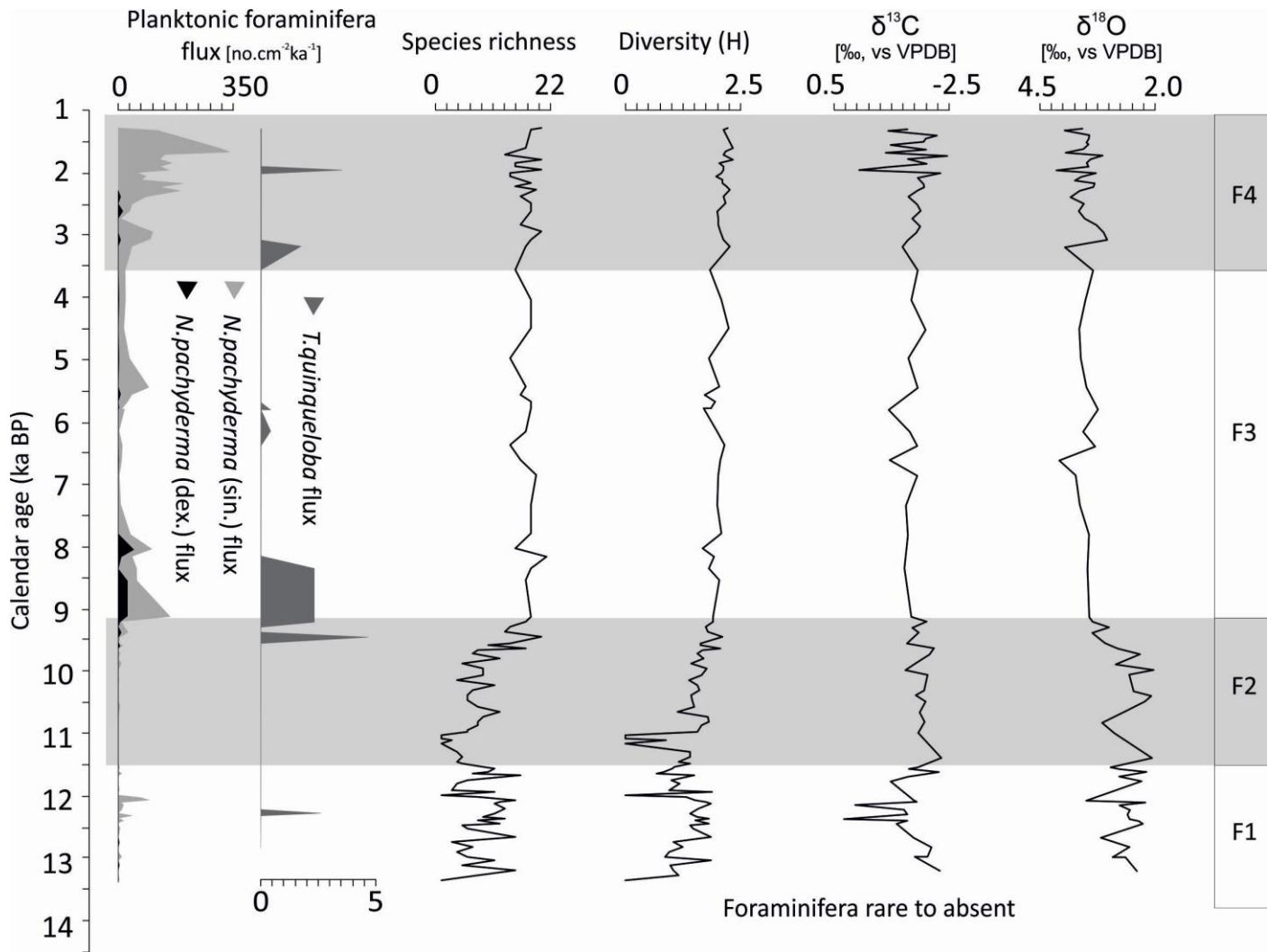
1136



1138  
1139

1140 Fig. 5. Percentage distributions (upper scale; black line) and fluxes (no. cm<sup>-2</sup> ka<sup>-1</sup>; bottom  
1141 scale; grey shading) of the most dominant benthic foraminiferal species plotted versus  
1142 thousands of calendar years with indicated foraminiferal zonation (zones F1-F4) and  
1143 lithostratigraphic units (L1-L4). Foraminiferal taxa are grouped based on their ecological  
1144 tolerances described in the text.

1145



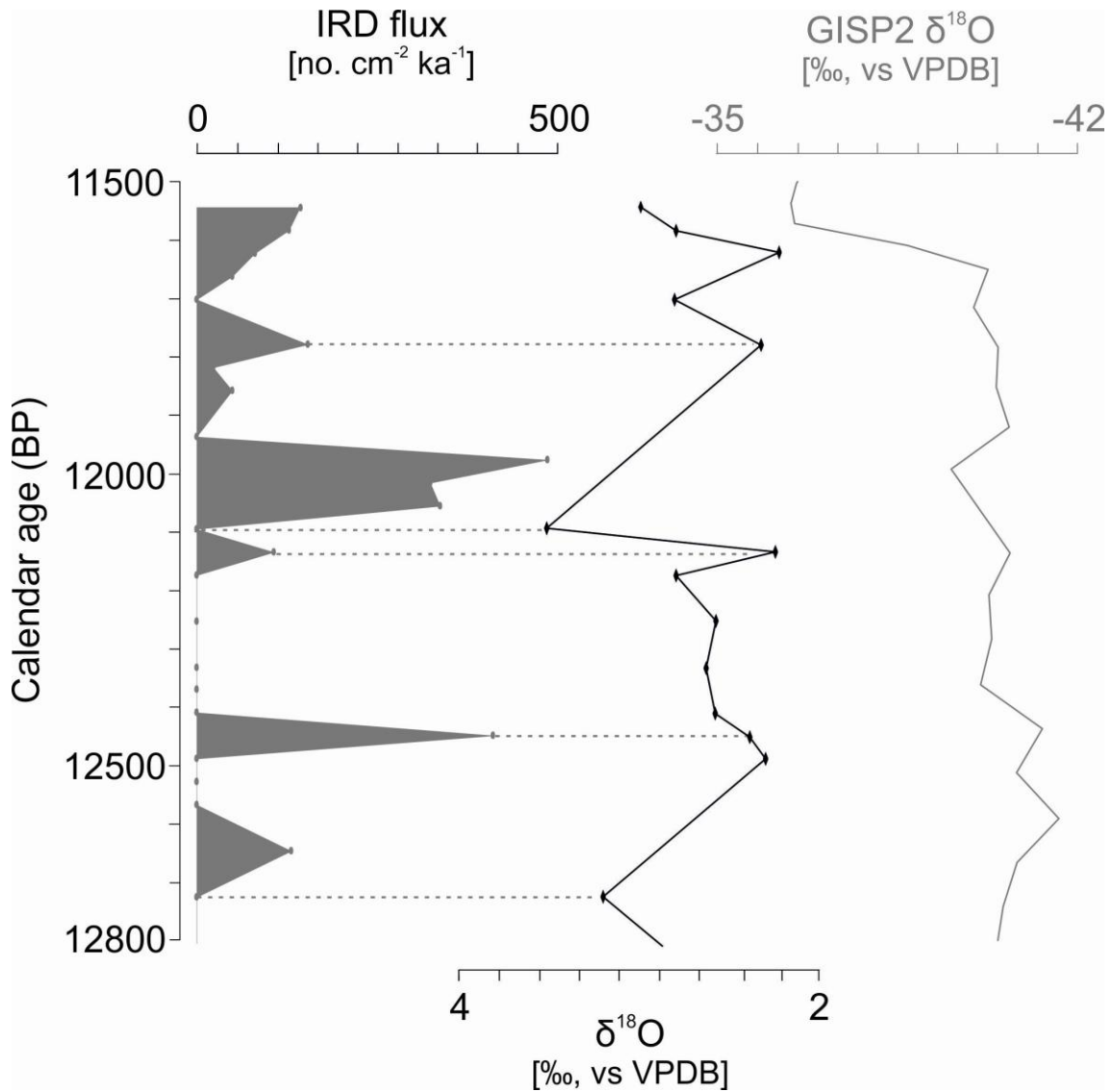
1146

1147

1148 Fig. 6. Fluxes of planktonic foraminifera ( $\text{no.cm}^{-2}\text{ka}^{-1}$ ), diversity parameters (species richness  
 1149 and Shannon - Wiener index) and stable oxygen and carbon isotope data ( $\delta^{18}\text{O}$  and  $\delta^{13}\text{C}$ )  
 1150 plotted versus thousands of calendar years. The foraminiferal zonation (zones F1-F4) and  
 1151 lithostratigraphic units (L1-L4) are indicated.

1152



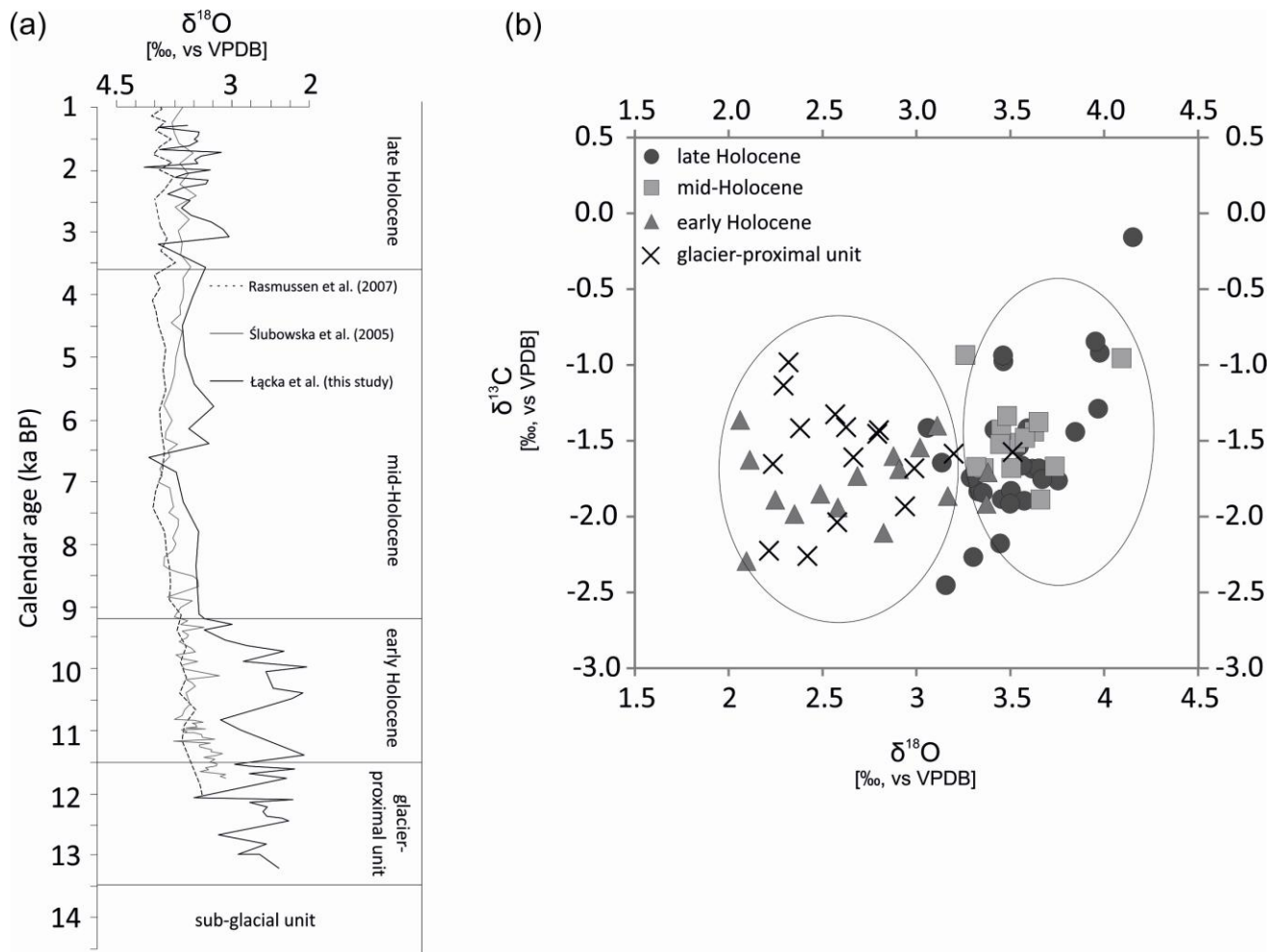


1153

1154

1155 Fig. 7 IRD flux (upper scale, grey shading) and oxygen stable isotopes records (bottom scale,  
 1156 black line) compared with oxygen stable isotopes records from ice core GISP2 from  
 1157 Greenland during the Younger Dryas period (12,800 cal yr BP to 11,500 cal yr BP).

1158



1159  
1160

1161 Fig. 8 (a) The comparison of  $\delta^{18}\text{O}$  records (corrected for ice volume changes) between Łącka  
 1162 et al. (this study; black solid line) and Ślubowska et al. (2005; grey solid line) and Rasmussen  
 1163 et al. (2007; black dashed line) plotted versus thousands of calendar years. The  $\delta^{18}\text{O}$  records  
 1164 after Łącka et al. (this study) were measured on *E.excavatum* f. *clavata* and the two latter ones  
 1165 (Ślubowska et al., 2005 and Rasmussen et al., 2007) were measured on *M.barleeanum*. (b)  
 1166 Scatter plot showing  $\delta^{13}\text{C}$  versus  $\delta^{18}\text{O}$  values from core JM09-020-GC (this study).

1167